Distinct endocytic pathways regulate TGF-β receptor signalling and turnover

Gianni M. Di Guglielmo*, Christine Le Roy*, Anne F. Goodfellow and Jeffrey L. Wrana†

Programme in Molecular Biology and Cancer, Samuel Lunenfeld Research Institute, Mount Sinai Hospital, Toronto, Canada
**These authors contributed equally to this work.*
†e-mail: wrana@mshri.on.ca

Published online: 28 April 2003, DOI 10.1038/ncb975

Endocytosis of cell surface receptors is an important regulatory event in signal transduction. The transforming growth factor β (TGF-β) superfamily signals to the Smad pathway through heteromeric Ser-Thr kinase receptors that are rapidly internalized and then downregulated in a ubiquitin-dependent manner. Here we demonstrate that TGF-β receptors internalize into both caveolin- and EEA1-positive vesicles and reside in both lipid raft and non-raft membrane domains. Clathrin-dependent internalization into the EEA1-positive endosome, where the Smad2 anchor SARA is enriched, promotes TGF-β signalling. In contrast, the lipid raft-caveolar internalization pathway contains the Smad7-Smurf2 bound receptor and is required for rapid receptor turnover. Thus, segregation of TGF-β receptors into distinct endocytic compartments regulates Smad activation and receptor turnover.

In higher eukaryotic cells, internalization of plasma membrane proteins and lipids is mediated by clathrin-dependent and independent pathways[1] and after internalization the intracellular itinerary of receptors regulates signal transduction[2–4]. Clathrin-mediated endocytosis targets proteins to the early endosome and is an important pathway for downregulating many receptors through ubiquitin-dependent sorting processes involving ubiquitin binding proteins resident in the clathrin pathway[5]. Non-clathrin-dependent endocytosis through lipid raft and caveolar pathways has recently emerged as another important trafficking pathway[6]. Lipid rafts are cholesterol- and sphingolipid-rich domains in the membrane[7,8], a subpopulation of which form membrane invaginations called caveolae that are rich in caveolin protein[7,8]. Lipid rafts and caveolae function in vesicular and cholesterol trafficking[9,10] as well as internalization of toxins, SV40 virus and glycosyl phosphatidylinositol (GPI)-anchored proteins[6,9,11,12] and regulate the internalization of autocrine motility factor (AMF) receptor[13]. Furthermore, rafts can control a variety of signalling pathways[14–16], but it is unclear if they function in controlling receptor downregulation.

TGF-β superfamily members signal through heteromeric complexes of type II and type I transmembrane Ser-Thr kinase receptors[17]. In the prototypic TGF-β pathway, ligand induces the assembly of a heteromeric receptor complex, within which the TGF-β type II receptor (TβRII) transphosphorylates and activates the type I receptor (TβRI)[18]. TβRI in turn initiates Smad signalling[19] by phosphorylating the receptor-regulated Smads, R-Smad2 and R-Smad3, and this is facilitated by the Smad anchor protein called Smad anchor for receptor activation (SARA), which also binds the receptors and contains a Fab1p, YOTB, Vac1p and EEA1 (FYVE) domain, which binds to membranes through specific interactions with phosphatidyl inositol 3′ phosphate (PtdIns(3)P; ref 20). Once phosphorylated, R-Smads associate with Smad4 and accumulate in

Table 1 Quantitation of TGF-β receptor distribution by immunoelectron microscopy[a]

Embedding medium	Treatment	Time[b] (min)	At the cell surface	In caveolin-1-negative vesicles	In caveolin-1-positive vesicles	Total
LR White	–TGF-β	15	18 (8%)	125 (52%)	97 (40%)	240 (100%)
		60	7 (3%)	117 (54%)	93 (43%)	217 (100%)
	+TGF-β	15	9 (6%)	73 (46%)	76 (48%)	158 (100%)
		60	ND	201 (49%)	210 (51%)	411 (100%)
Lowicryl	–TGF-β	15	30 (4%)	426 (57%)	291 (39%)	747 (100%)
		60	29 (3%)	497 (56%)	355 (40%)	881 (100%)
	+TGF-β	60	2 (1%)	114 (53%)	98 (46%)	214 (100%)
Control[c] Lowicryl	–TGF-β	15	2 (2%)	124 (98%)	0 (0%)	126 (100%)
		60	8 (4%)	201 (96%)	0 (0%)	209 (100%)

[a] TβRII labelled with gold conjugated antibodies in the indicated compartments were counted. Counts were derived from 2 LR White and 2 Lowicryl experiments with a total of 3213 gold particles counted in 75 cells
[b] Internalization time at 37°C
[c] Control labelling was determined in the absence of caveolin-1 antibody

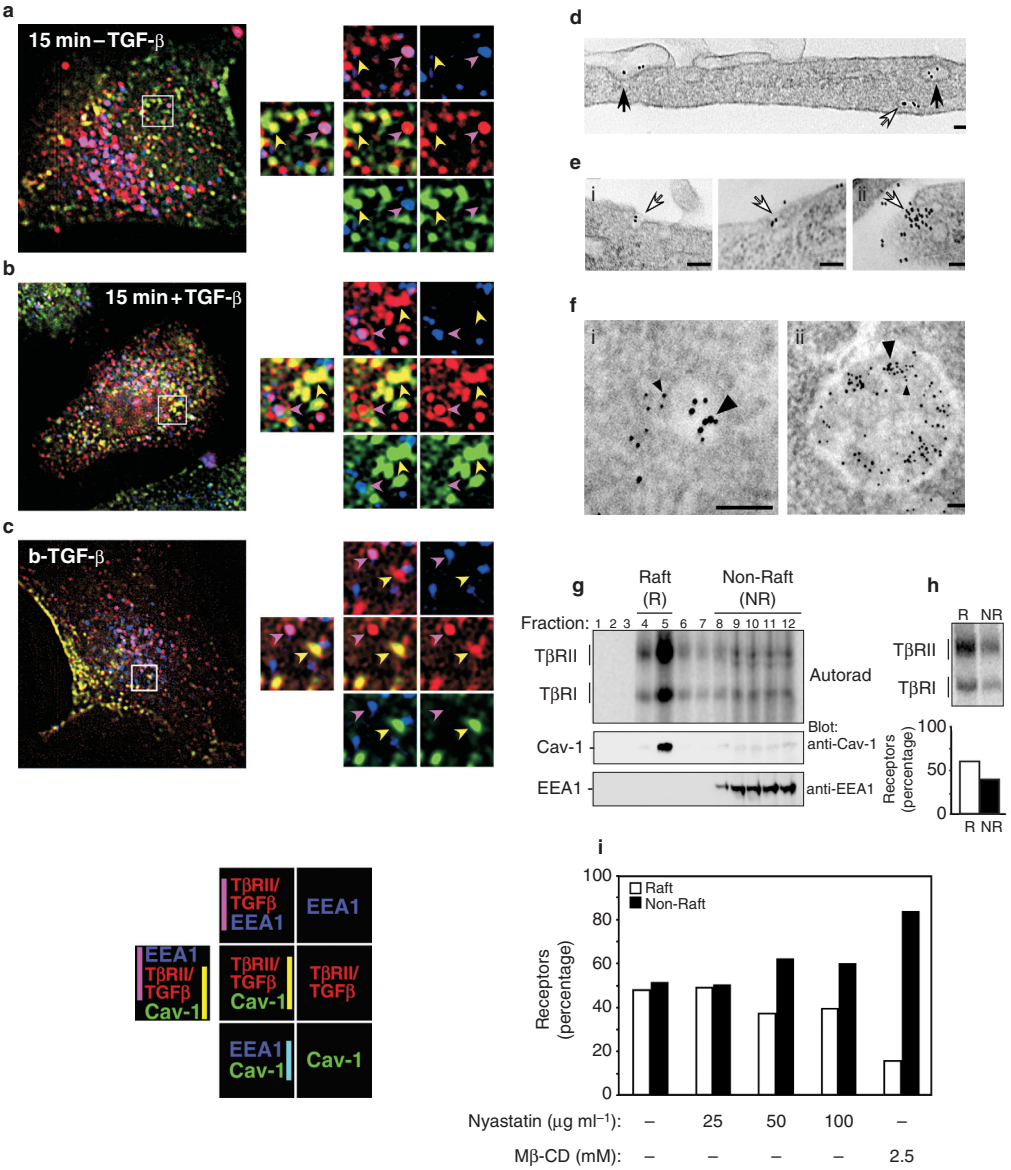

Figure 1 **TGF-β receptors localize to both Cav-1 and EEA1 positive compartments.** Mv1Lu cells expressing extracellularly HA-tagged TβRII receptors were incubated with mouse anti-HA Fab fragments followed by Cy3-conjugated donkey-anti-mouse Fab fragments (**a**, **b**), washed and incubated at 37 °C for 15 min in the absence (**a**) or presence (**b**) of TGF-β. **c**, Cells were labelled with biotinylated TGF-β (b-TGF-β) and Cy3-conjugated stretavidin. After fixation, EEA1 was detected using an anti-EEA1 monoclonal antibody, followed by a FITC-conjugated anti-mouse, Fc-specific secondary. Caveolin was detected using a rabbit anti-Cav-1 antibody and Cy5-conjugated anti-rabbit antibody. Images were collected and processed by deconvolution microscopy. EEA1, receptors (**a**, **b**) or b-TGF-β (**c**) and caveolin staining are coloured blue, red and green, respectively, as indicated in the key and a representative area from each cell that displays receptors or b-TGF-β in the EEA1 (purple arrowhead) and caveolin-1 (yellow arrowhead) compartments is enlarged. The staining combinations shown in the enlarged section are summarized in the key along with the expected colours observed due to costaining (vertical bars). Co-localization of receptors or b-TGF-β (red) with EEA1 (blue) appears as purple, whereas co-localization of receptors with caveolin-1 (green) is yellow. Significant co-localization of EEA1 and caveolin was not observed but would appear as aquamarine. **d–f** Ultrastructural and immunoelectron microscopic analysis of TGF-β receptor trafficking was carried out in HA–TβRII expressing Mv1Lu cells. Receptors were labelled as described above using secondary antibodies conjugated to 10 nm colloidal gold. After incubation at 37 °C for 5 min, cells were fixed, processed for optimal morphology and visualized by electron microscopy (**d**, **e**). **f**, For immunoelectron microscopy, cells in which receptors were labelled with 10 nm gold were incubated for 15 min (i) or 60 min (ii) at 37 °C and processed for post-embedding immunogold labelling with anti-caveolin-1 antibodies followed by secondary antibodies conjugated to 6 nm colloidal gold. Black arrows indicate 10 nm gold-labelled receptors in a clathrin-coated pit and vesicle (**d**) and white arrows mark receptors in a smooth vesicle (**d**) or caveolar-like membrane invaginations (**e**, i–iii). **f**, Large arrowheads indicate 10 nm colloidal gold-labelled TβRII and the small arrowheads indicate 6 nm gold-labelled caveolin-1. Bars, 100 nm. **g–i** TGF-β receptor distribution in lipid raft and non-raft fractions was analysed in Mv1Lu cells affinity labelled with [^{125}I]-labelled TGF-β and subjected to sucrose gradient subcellular fractionation to separate lipid rafts from other cellular components. **g**, An equal volume from each fraction was analysed by SDS-PAGE electrophoresis followed by autoradiography or western blotting with anti-caveolin-1 (Cav-1) or anti-EEA1 antibodies. **h**, Fractions containing rafts (fractions 4 and 5) or EEA1 (fractions 8–12) were pooled, immunoprecipitated with anti-TβRII antibodies, subjected to SDS-PAGE, autoradiography and quantification by phosphorimaging. To disrupt rafts Mv1Lu cells were incubated in control media or media supplemented with the indicated concentrations of Nystatin or methyl-β-cyclodextrin (Mβ–CD) before affinity labelling with [^{125}I]-TGF-β. **i**, Following a 2 h chase at 37 °C receptors were fractionated on sucrose gradients and quantified by phosphorimaging as described above.

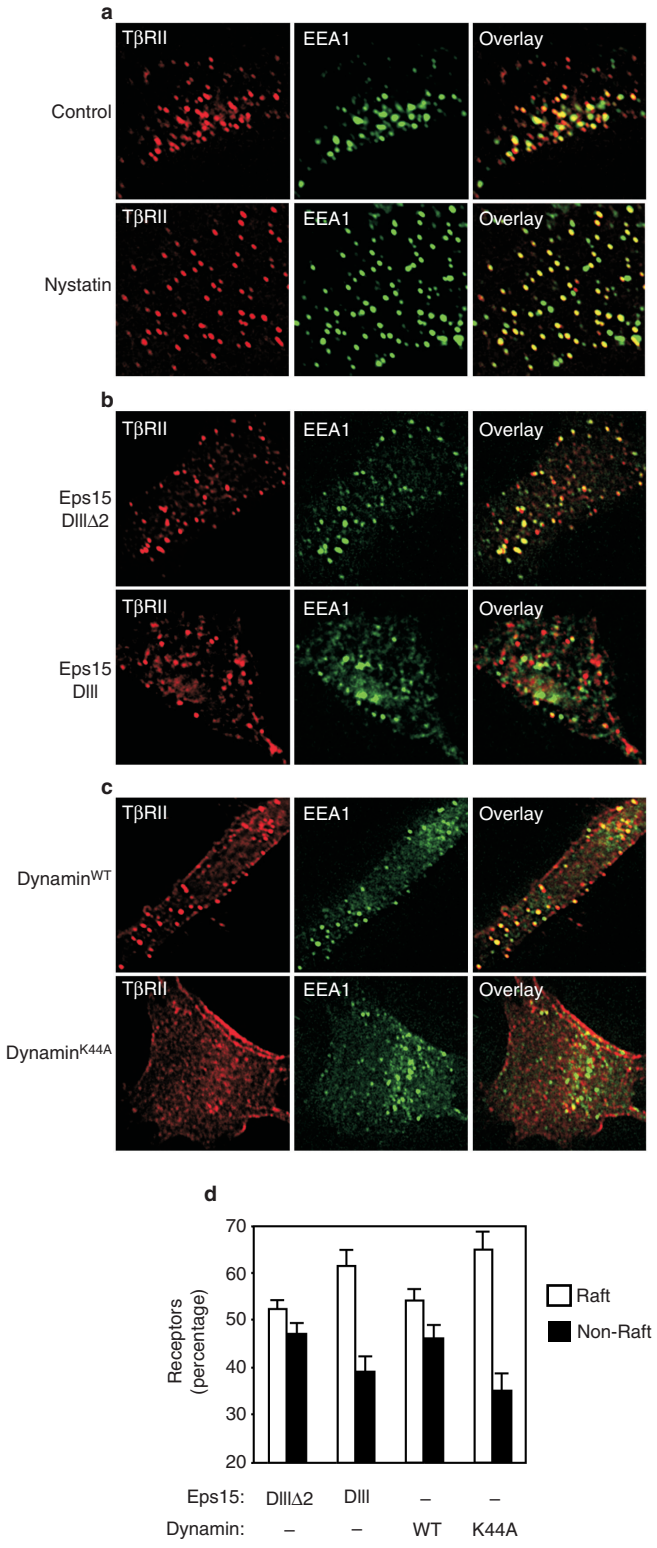

Figure 2 **Dominant negative mutants of Dynamin or Eps15 modulate TGF-β receptor colocalization in subcellular compartments. a**, Mv1Lu cells expressing extracellularly HA-tagged TGF-β type II receptors (red) were incubated in control media or media containing 50 μg ml^{-1} Nystatin and processed for receptor internalization studies using anti-HA Fab fragments as described in Fig. 1. Alternatively, cells were transiently transfected with **b**, cDNA encoding control Eps15 (DIIIΔ2) or a dominant negative form of Eps15 (DIII); or **c**, wild type Dynamin (WT) or a dominant negative mutant of Dynamin (K44A,) and then processed for receptor internalization studies as described above. **d**, HEK 293T cells were transiently transfected with cDNA encoding TGF-β type I and II receptors, an Eps15 control (DIIIΔ2) or dominant negative mutant (DIII), with wild type Dynamin (WT) or dominant negative Dynamin (K44A) and subjected to affinity labelling, sucrose gradient subcellular fractionation, SDS-PAGE autoradiography and quantification as described in Fig. 1.

the nucleus to regulate gene transcription[19]. The inhibitory Smad — Smad7 — negatively regulates TGF-β signalling by interacting with TβRI[21–23] and recruiting the E3 ligases, Smurf1 and Smurf2, which direct ubiquitin-dependent degradation of the TGF-β receptor-Smad7 complex[24,25].

The internalization pathway of TGF-β receptors remains unclear. Receptor internalization through the clathrin pathway[26,27] may be important for signalling[27,28] and SARA has been found in the PtdIns(3)P-enriched early endosome antigen-1 (EEA1)-positive endosomes[27,29,30] that are downstream of this route. However, caveolin-1 has been shown to bind TβRI[31] and another study suggests that receptors can internalize through a non-clathrin-dependent pathway[32]. Here we show that TGF-β receptors are internalized by both clathrin- and caveolin-1-lipid raft-dependent pathways. We demonstrate that although receptor internalization into the EEA1-positive compartment facilitates Smad2 signalling, Smad7–Smurf2-dependent receptor degradation is dependent on lipid raft-caveolar pathways. Furthermore, we suggest that clathrin-dependent trafficking functions to promote signalling by sequestering receptors from the raft-caveolar compartment. Thus compartmental segregation of TGF-β receptors during endocytosis regulates signal transduction and receptor turnover.

Results

TGF-β receptors internalize through clathrin-coated pits and caveolae. To examine trafficking of TGF-β receptors we generated Mv1Lu clones that inducibly express TβRII modified to contain an extracellular haemagglutinin (HA) tag. Tagged receptors on the cell surface were then labelled at 4 °C using anti-HA antibodies and fluorescent-conjugated secondary antibodies. Trafficking was then initiated by incubating at 37 °C and the internalization compartments analysed by three colour immunofluorescence to simultaneously label the receptors, EEA1 (a marker of the early endosome) and caveolin-1 (a marker of the raft-caveolar pathway) in the same cell. These studies revealed that the majority of internalized receptors colocalized with either EEA1 (purple) or caveolin-1 (yellow) after both 15 and 60 min of incubation (Fig. 1a and data not shown). Similar results were obtained using either Fab fragments or whole Immunoglobulin-γ (IgG) to label the receptor. Further analysis also revealed little colocalization of caveolin-1 and EEA1 (aquamarine), consistent with these representing distinct compartments[11,12]. We also analysed trafficking of the receptor in the presence of TGF-β ligand, but observed no appreciable difference between treated and untreated cells, as reported previously[26](Fig. 1b).

Next, we examined whether TGF-β also trafficked into both compartments using biotinylated TGF-β (b-TGF-β). Similar to HA–TβRII, b-TGF-β colocalized with both the caveolin and EEA1 compartments (Fig. 1c) and was also observed in both compartments in cells not expressing cell-surface HA–TβRII (Supplementary Information, Fig.S1a). This suggests that ligand-bound endogenous receptor and antibody-labelled HA–TβRII follow similar trafficking routes. To confirm this, we examined b-TGF-β and Fab-labelled HA–TβRII in the same cell. HA–labelled TβRII and b-TGF-β showed extensive colocalization (yellow staining) and these ligand- and receptor-labelled compartments colocalized with either caveolin or EEA1 (white staining) (Supplementary Information, Fig. S1b). Thus, TGF-β and

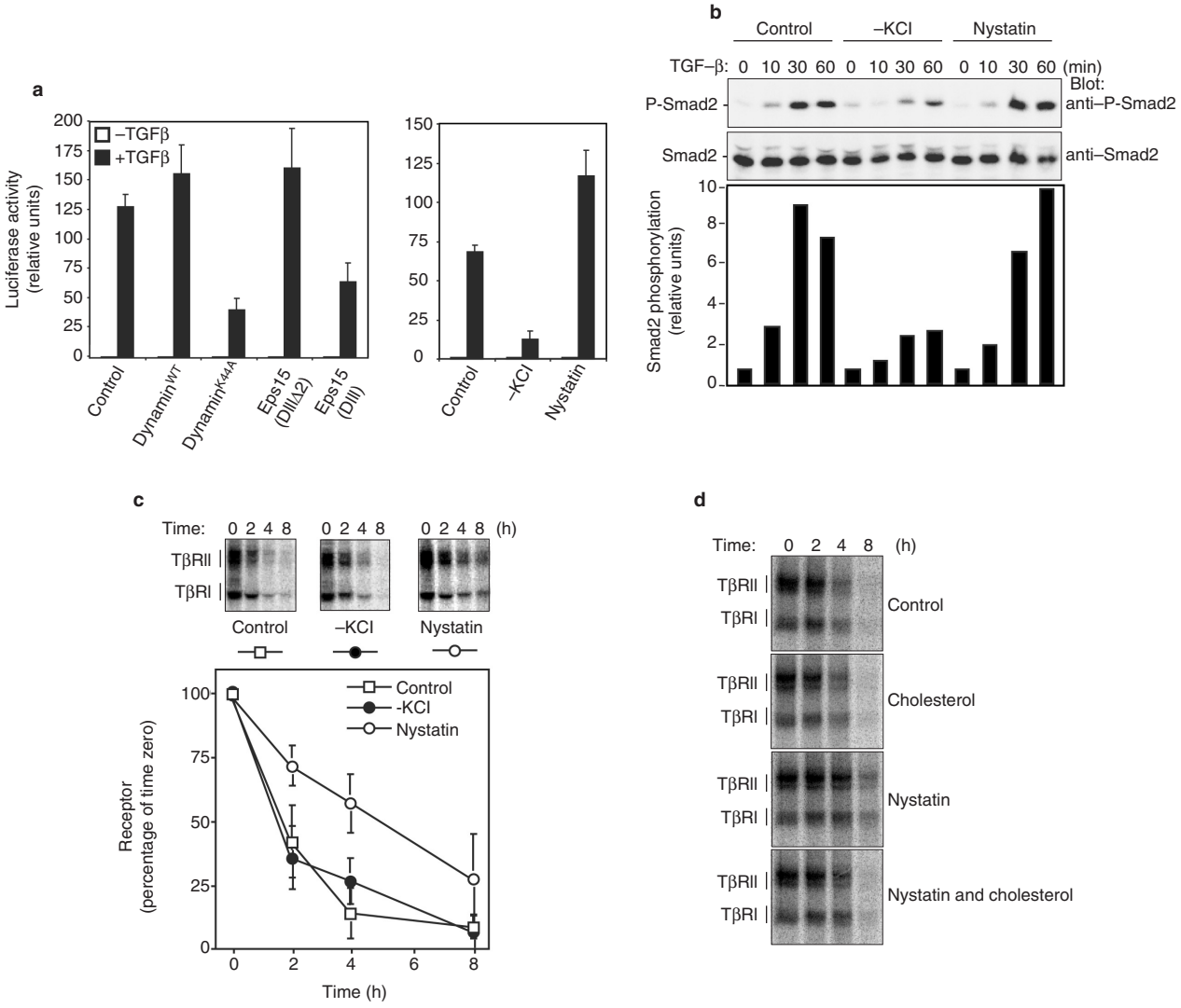

Figure 3 **TGF-β receptor signal transduction and turnover is dependent on distinct subcellular compartments. a**, HepG2 cells were transiently transfected with FoxH1, A3-lux and either Eps15 control (DIIIΔ2) or dominant negative Eps15 (DIII), wild-type Dynamin (WT) or dominant negative Dynamin (K44A) and incubated with or without 100 pM TGF-β (left). Alternatively, HepG2 cells transiently transfected with FoxH1 and A3-lux were incubated in control media (control), media lacking potassium chloride (–KCl) or media supplemented with 50 μg ml^{-1} Nystatin (Nystatin) in the presence or absence of 100 pM TGF-β (right). Luciferase activity was normalized to β-galactosidase activity and plotted as the mean ± SD of triplicates from a representative experiment. **b**, Mv1Lu cells incubated in media as described (Fig. 3a) were treated for the indicated times with 0.5 nM TGF-β and processed for immunoblotting with anti-phospho-specific Smad2 (anti–P-Smad2) or Smad2 antibodies (anti–Smad2). The signal corresponding to the phospho-Smad2 bands (normalized to the amount of Smad2 in each lane) was carried out and represented below the immunoblots. **c**, Mv1Lu cells were incubated in media described (Fig. 3a) and receptors were affinity-labelled using [^{125}I]-labelled TGF-β at 4 °C followed by cross-linking. Following incubation at 37 °C for the indicated times, cells were lysed, processed for SDS-PAGE and endogenous receptors were visualized by autoradiography (top). Three separate experiments were carried out, quantified by phosphorimaging and graphed as receptor quantity (% of time 0) vs. time. Each point represents the mean ± SD. **d**, Mv1Lu cells were incubated in control media or media containing 25 μg/ml of cholesterol, Nystatin or cholesterol and Nystatin and receptors were affinity-labelled using [^{125}I]-labelled TGF-β at 4 °C followed by cross-linking. Following incubation at 37 °C for the indicated times, cells were lysed, processed for SDS-PAGE and endogenous receptors were visualized by autoradiography.

HA–TβRII follow similar trafficking routes.

Transmembrane proteins in the EEA1 compartment can enter either the late endosome-lysosome for degradation, or the Rab11-positive recycling endosome[33]. Thus we analysed p62, a marker of the late endosome[34], but observed little or no co-localization with receptors, whereas some receptor-containing vesicles colocalized with Rab11 (Supplementary Information Fig. S2), suggesting that receptors in the EEA1 compartment can recycle back to the cell surface. Entrance to the EEA1-positive compartment occurs through clathrin-mediated endocytosis[35]. In contrast, caveolin-positive vesicles arise from caveolae and represent a non-clathrin internalization pathway[11]. To verify that TGF-β receptors internalize through both pathways, cell surface receptors were labelled with 10 nm colloidal gold, allowed to internalize for 5 min, and analysed by electron microscopy. Under these conditions HA-tagged receptors were detected at the cell surface and accumulated in clathrin-coated pits and vesicles (Fig. 1d; Supplementary Information Fig. S3a and b,

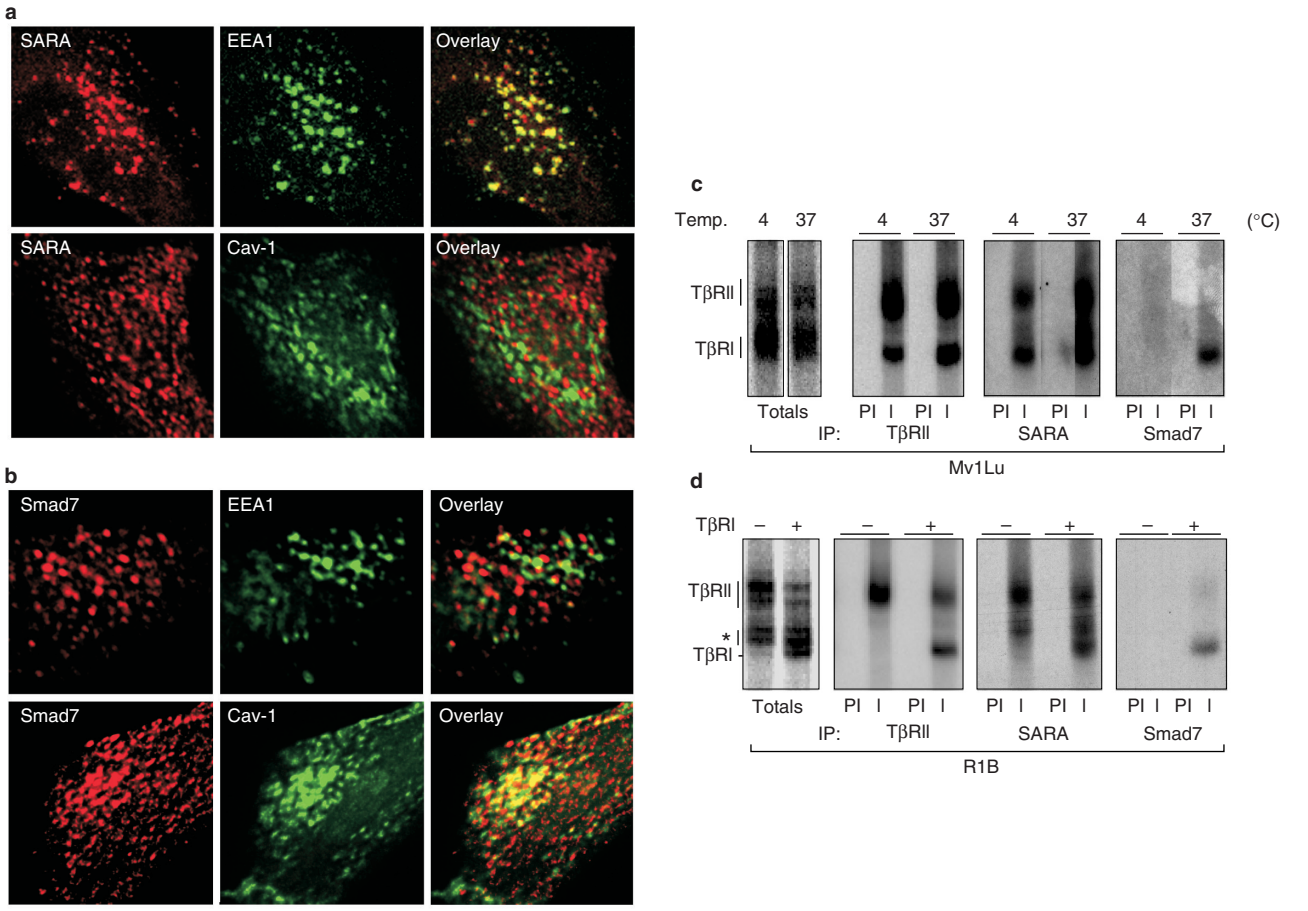

Figure 4 **SARA and Smad7 (Smurf2) localize to distinct subcellular Ocompartments. a**, Mv1Lu cells transiently transfected with SARA were fixed and probed with goat anti-SARA (red) and mouse anti-caveolin-1 (Cav-1; green) or anti-EEA1 (green) antibodies. **b**, Mv1Lu cells transiently transfected with HA-tagged Smad7 (red) and myc-tagged catalytically inactive Smurf2 CA were probed with anti-HA and anti-EEA1 (green) or anti-caveolin-1 (Cav-1) (green) antibodies. Both **a** and **b** were visualized by deconvolution immunofluorescence microscopy. **c**, Mv1Lu cells were affinity-labelled with [^{125}I]-TGF-β at 4 °C for 2 h or 37 °C for 1 h, cross-linked and cell lysates were subjected to immunoprecipitation with pre-immune antisera (PI) or immune sera (I) raised to TβRII, SARA or Smad7. Samples were subjected to SDS-PAGE and receptors were visualized by autoradiography. **d**, Parental R1B or R1B cells expressing TβRI were labelled with [^{125}I]-TGF-β at 37 °C for 1 h, cross-linked and processed as described in panel c. The asterisk (*) indicates bands that migrate between the type II and type I receptors and may represent fragments of TβRII.

ii). Additionally, we detected receptors in 50–75 nm diameter non-clathrin coated invaginations and vesicles that displayed morphologies ranging from flask-like (Fig. 1e, i and ii; Supplementary Information Fig. S3b, i) to grape-like (Fig. 1e, iii; Supplementary Information Fig. S3b, ii), similar to previous reports for caveolar structures[11,16]. Quantitation revealed that after 5 min at 37 °C, 28% of cell surface-labelled receptors were in non-clathrin-coated structures, 20% were in clathrin-coated structures and 52% were still at the plasma membrane (of 531 gold particles counted).

Caveolin-containing vesicles cannot be unambiguously identified based on their morphology, so we performed double-label immunoelectron microscopy. At 15 min after internalization, receptors were found in caveolin-1-containing structures roughly 75 nm in diameter (Fig. 1f, i), but after 60 min we observed them in larger structures (400–500 nm; Fig. 1f, ii; Supplementary Information Fig. S3c), some of which were electron lucent whereas others resembled multivesicular bodies or were irregularly shaped, as previously reported[11,16]. We next quantified receptors in caveolin-1 structures using either LR white or Lowicryl embedding (Table 1). After 15 min at 37 °C, 94% of cell surface-labelled receptors were internalized with 40% in caveolin-1-positive vesicles compared to 42% at 60 min. As noted above, TGF-β caused no substantial shift in receptor partitioning (Table 1 and data not shown).

Caveolin associates with cholesterol- and sphingolipid-rich membrane domains called lipid rafts[7,8], suggesting that TGF-β receptors also reside in these membranes. To verify this, we affinity-labelled endogenous TGF-β receptors with [^{125}I]-TGF-β and fractionated rafts by sucrose density centrifugation[36]. Autoradiography (Fig. 1g) and quantitation (Fig. 1g) demonstrated that receptors were in the raft (55%) and non-raft fraction, which contained caveolin-1 or EEA1, respectively. Furthermore, disruption of cholesterol using methyl-β-cyclodextrin (Mβ-CD) or Nystatin[8] shifted receptors into the non-raft compartment (Fig. 1i), confirming that receptor presence in the low-density fraction was dependent on rafts. Altogether these data demonstrate that TGF-β receptors reside in raft and non-raft membrane domains and internalize into distinct endocytic compartments — the EEA1-positive early endosome and caveolin-positive structures.

Dynamic regulation of TGF-β receptor trafficking and membrane compartmentalization. To examine the dynamics of receptor traf-

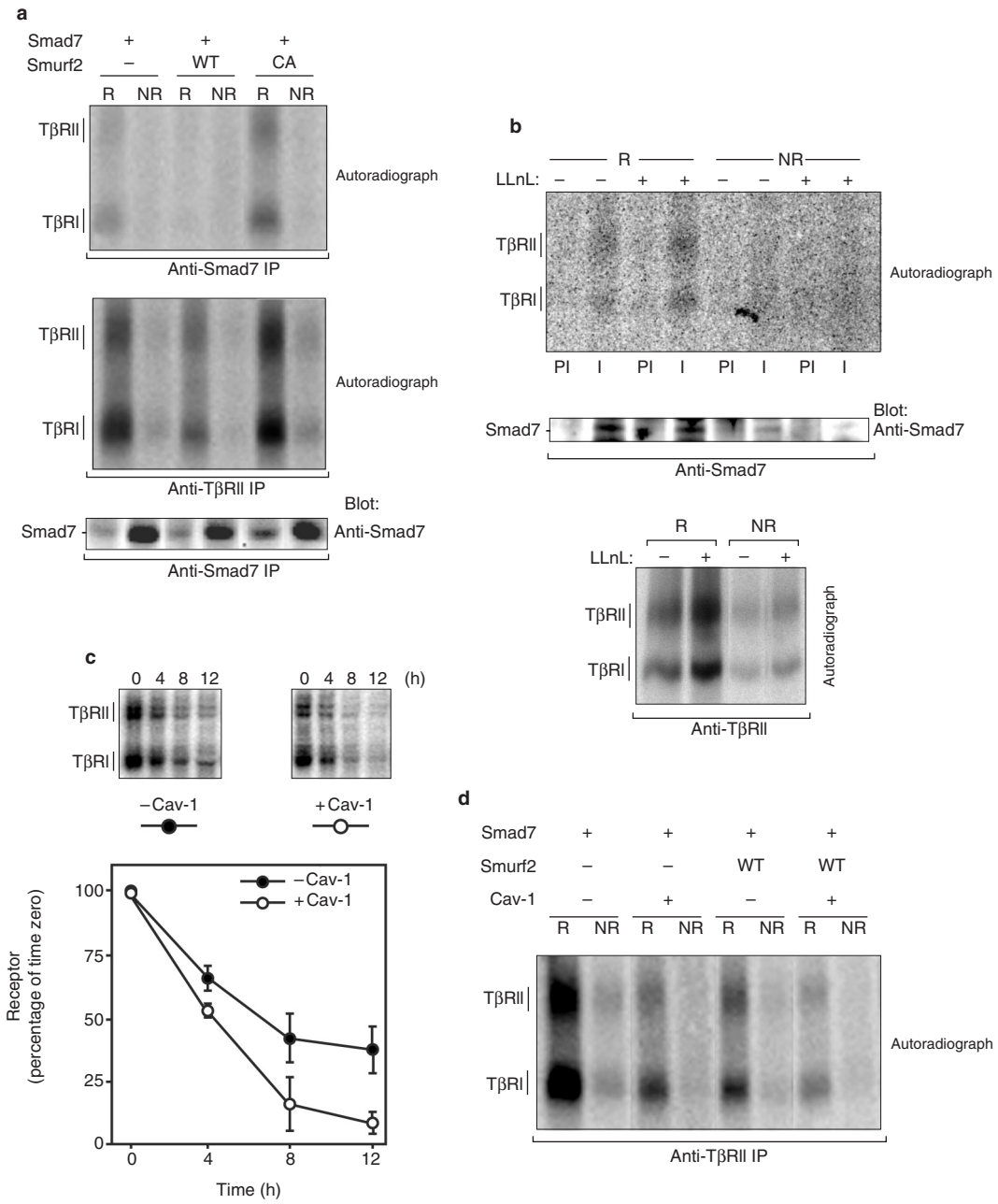

Figure 5 **Receptor binding proteins that associate with raft fractions stimulate receptor complex turnover. a**, HEK 293T cells transiently transfected with TβRI and TβRII in combination with Smad7 in the absence or presence of wild type Smurf2 (WT) or an ubiquitin ligase-deficient Smurf2 (CA) were affinity-labelled with [^{125}I]-TGF-β and subjected to sucrose density subcellular fractionation. The Raft (R) and Non-Raft (NR) fractions were pooled and immunoprecipitated with anti-Smad7 or TβRII antibodies and subjected to SDS-PAGE and autoradiography or immunoblotting with anti-Smad7 antibodies. **b**, Mv1Lu cells were incubated in control media or media containing the proteasomal inhibitor LLnL and receptors were affinity-labelled with [^{125}I]-TGF-β and subjected to sucrose density subcellular fractionation. The Raft (R) and Non-Raft (NR) fractions were pooled and immunoprecipitated with pre-immune (PI) or anti-Smad7 or TβRII antibodies and subjected to SDS-PAGE and autoradiography or immunoblotting with anti-Smad7 antibodies. **c**, HEK 293T cells were transiently transfected with TGF-β type I and type II receptors in the absence or presence of caveolin-1 (Cav-1) and subjected to affinity-labelling, chased for the indicated times and processed for SDS-PAGE and autoradiography (top). Three separate experiments were carried out, quantified by phosphorimaging and graphed as receptor quantity (% of time 0) vs. time. Each point represents the mean ± SD. **d**, HEK 293T cells transiently transfected with TβRI and TβRII in combination with Smad7 and wild type Smurf2 (WT) and/or caveolin-1 (Cav-1) were affinity-labelled with [^{125}I]-TGF-β and subjected to sucrose density subcellular fractionation. The Raft (R) and Non-Raft (NR) fractions were pooled and immunoprecipitated with anti-TβRII antibodies and subjected to SDS-PAGE and autoradiography.

ficking, we next evaluated whether interfering with either pathway would shift the receptors into the alternative pathway. Disrupting rafts using Nystatin caused the majority of receptors to enter the EEA1 compartment (79 ± 4% in the Nystatin-treated cells against 46 ± 1% in the controls, Fig. 2a). As Mβ-CD strips cholesterol from the membrane and blocks clathrin endocytosis[37,38], we confirmed (using Mv1Lu cells) previous reports[39,40] that Nystatin does not interfere with clathrin-dependent endocytosis by analyzing trans-

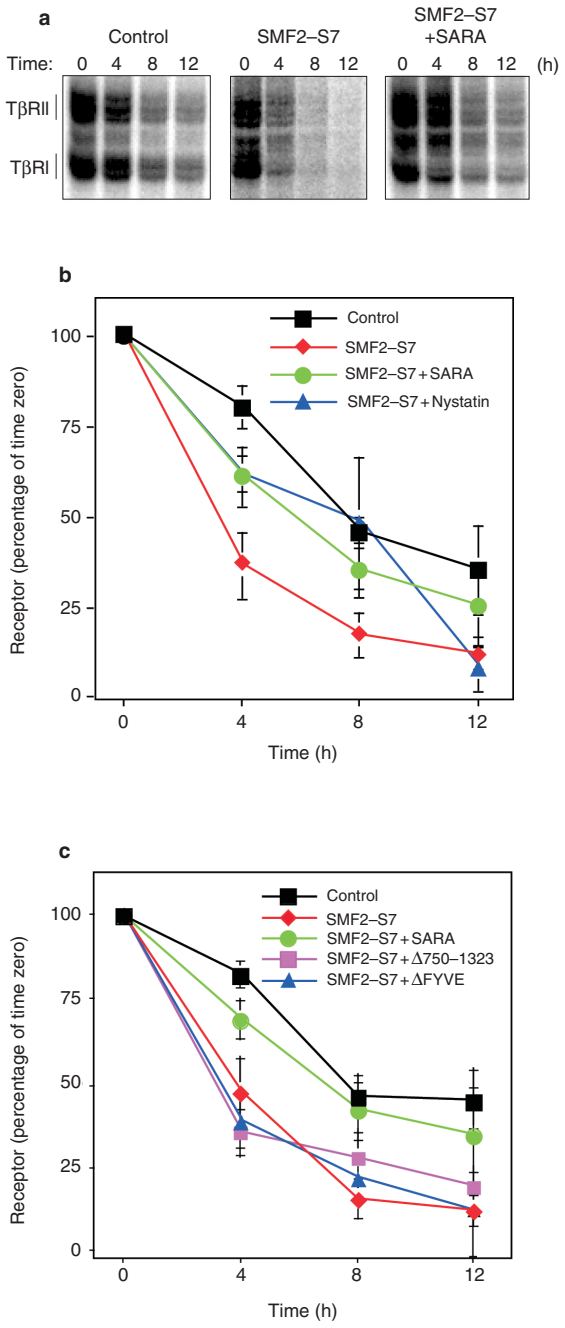

Figure 6. **SARA interferes with receptor complex degradation. a**, HEK 293T cells transiently transfected with TβRI and TβRII in combination with Smad7–Smurf2 (SMF2–S7) and SARA were incubated with [^{125}I]-labelled TGF-β, cross-linked and incubated for the indicated times at 37 °C. Cell lysates were subjected to SDS-PAGE and visualized by autoradiography. **b**, Three separate experiments were carried out as described in **a** and quantified by phosphoimaging. The quantity of receptor (% of time 0) vs. time (h) is indicated as the mean ± SD. The time course of receptor turnover in the presence of Smad7–Smurf2 (SMF2–S7) and Nystatin (50 μg ml^{-1}) is also shown. **c**, HEK 293T cells overexpressing TβRI and TβRII in combination with Smurf2–Smad7 (SMF2–S7), SARA, SARA lacking the receptor binding domain (Δ750-1323) or SARA lacking the FYVE domain (ΔFYVE) were subjected to a [^{125}I]-TGF-β pulse chase as described in **a**. The receptor content was quantified by phosphorimaging and graphed as the mean ± SD.

ferrin endocytosis, which is a classic assay for this pathway (Supplementary Information Fig. S4a). We also examined b-TGF-β internalization and used acid washing to distinguish between membrane and internalized ligand (Supplementary Information Fig. S4b). As for receptors, Nystatin markedly increased localization of endocytosed b-TGF-β with EEA1.

Next, we assessed the localization of TβRII and b-TGF-β when clathrin-mediated endocytosis was inhibited. Dominant negative Eps15-DIII, which interferes with clathrin by binding to the AP-2 adaptor[41] (but not the inactive variant Eps15-DIIIΔ2) inhibited receptor entrance into the EEA1 compartment (Fig. 2b), as did K^+ depletion (data not shown), which prevents clathrin lattice assembly. Importantly, K^+ depletion, which completely blocked transferrin internalization (Supplementary Information Fig. S4a), did not block b-TGF-β internalization, but interfered with ligand entrance into the EEA1 compartment (Supplementary Information Fig. S4b). Thus receptor access to the EEA1-positive compartment requires clathrin-dependent trafficking. Finally, we examined dominant negative (DN) dynamin, which interferes with both clathrin-dependent and caveolae-dependent internalization[42,43]. Although wild type dynamin had no effect (Fig. 2c and data not shown), TGF-β receptors failed to internalize in cells expressing DN dynamin (Fig. 2c and data not shown). Altogether, these results demonstrate that TGF-β receptors endocytose through clathrin-dependent and non-clathrin-dependent endocytic pathways, both of which are dynamin sensitive.

As interfering with rafts caused enhanced clathrin-dependent internalization, we next asked whether interfering with clathrin-dependent endocytosis would alter receptor partitioning into the raft compartment. In control cells, about 50% of the receptors were present in the raft compartment and overexpression of Eps15-DIII — but not Eps15-DIIIΔ2 — induced 65% of the receptors to partition into the raft compartment (Fig. 2d). In addition, blocking all endocytosis using DN dynamin caused a similar shift of receptors into the raft fraction. Thus, interfering with clathrin-dependent endocytosis shifts TGF-β receptors into the raft compartment.

Altogether these data suggest that the membrane localization and trafficking of TGF-β receptors is dynamic and is controlled by distinct endocytic pathways.

Clathrin- and raft-dependent trafficking fulfill distinct functions in TGF-β signal transduction. To evaluate the importance of the clathrin and raft-caveolin pathways on the function and turnover of the TGF-β receptor, we first analysed TGF-β signalling using the Smad-dependent A3-lux reporter system. DN dynamin or Eps15-DIII inhibited TGF-β-dependent signalling, whereas wild type dynamin and Eps15-DIIIΔ2 had little effect (Fig. 3a). K^+-depletion also interfered with reporter gene activation (Fig. 3a) and TGF-β-dependent Smad2 phosphorylation (Fig. 3b). Similar effects of K^+ depletion and DN dynamin on TGF-β signalling have been reported[27,28], although others report minimal effects[44]. In contrast, interference with raft function using Nystatin slightly enhanced signalling and Smad2 activation. To assess endogenous receptor turnover, we followed cell surface receptors affinity labelled with [^{125}I]-TGF-β[25]. In K^+-depleted Mv1Lu cells the half-life ($t_{1/2}$) of the receptor complex was similar to the control (1.5 h; Fig. 3c), demonstrating that clathrin-dependent endocytosis is not required for TGF-β receptor turnover (Fig. 3c). In contrast, Nystatin treatment stabilized the receptors and increased their $t_{1/2}$ to approximately 4.5 h. This was dependent on chelation of cholesterol, as addition of cholesterol to Nystatin-treated cells restored rapid receptor turnover (Fig. 3d). These data indicate that clathrin-dependent endocytosis is important for TGF-β signalling through the Smad-dependent pathway, whereas rafts are required for rapid degradation of TGF-β receptors.

SARA and Smad7–Smurf2 localize to distinct endocytic pathways. To understand how differential trafficking of the TGF-β receptor into the EEA1 and caveolin-1 positive compartments regulates Smad signalling and receptor turnover, we focused on analyzing the

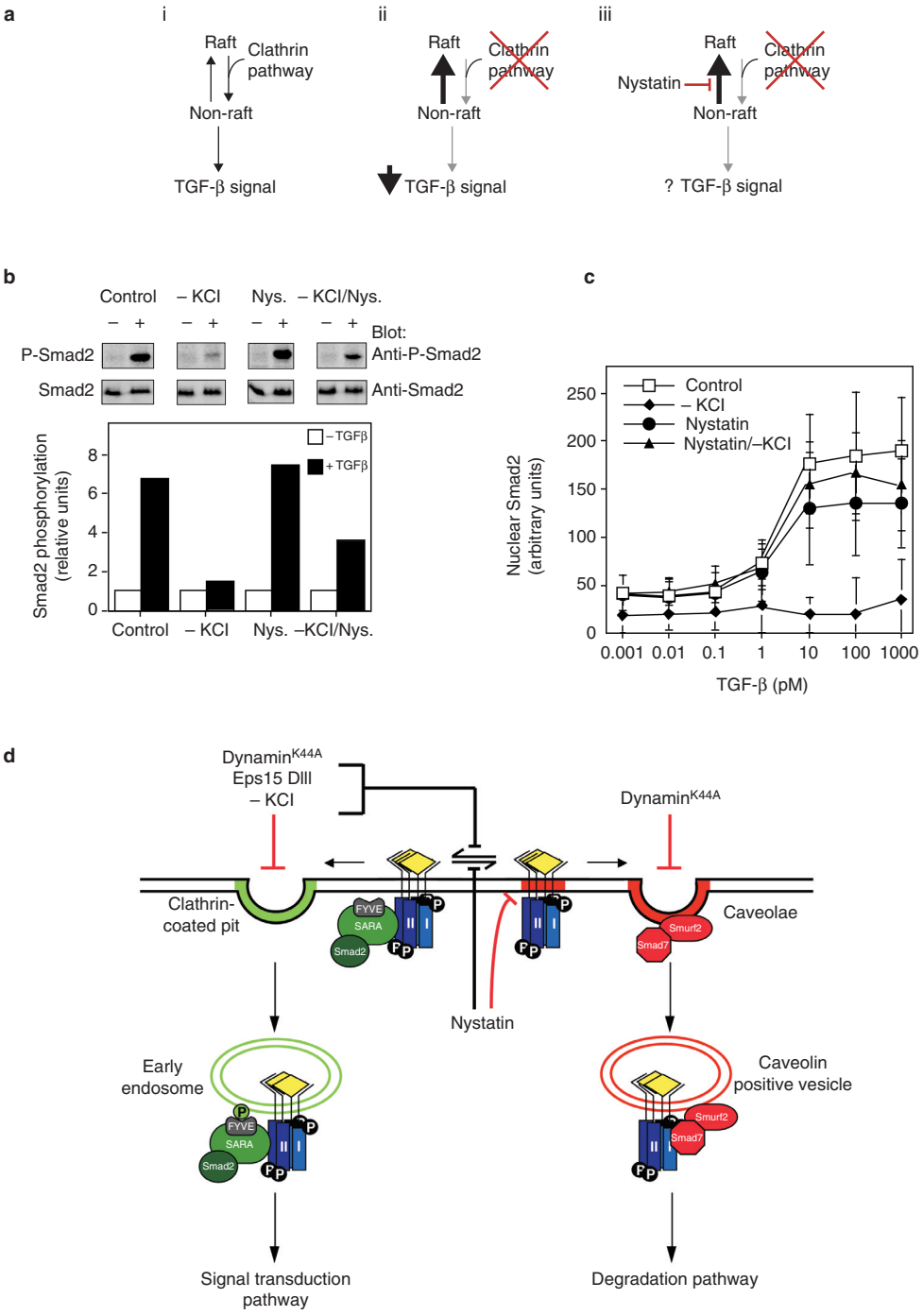

Figure 7 **Sequestering of TGF-β receptors from lipid rafts permits signal transduction. a**, Linear model for TGF-β signal transduction. The arrows indicate receptor movement into or out of the clathrin coated pit or the caveolae-lipid raft internalization pathways (i). Upon inhibition of clathrin-dependent endocytosis, receptors shift into the rafts (ii) and this correlates with reduced Smad activation. How Smad activation is affected when plasma membrane lipid rafts are disrupted in the presence of inhibitors of clathrin-dependent endocytosis is considered in the final panel (iii) and is assessed experimentally in panels **b** and **c**. **b**, Mv1Lu cells incubated in control media, media lacking potassium chloride (–KCl), media supplemented with 50 μg ml^{-1} Nystatin (Nys), or media lacking potassium chloride and containing Nystatin (–KCl/Nys) were treated with or without 0.5 nM TGF-β for 30 min and processed for immunoblotting with anti-phosphospecific Smad2 (anti-P-Smad2) or anti-Smad2 (anti–Smad2) antibodies. Quantitation of phosphorylated Smad2 is shown (bottom). **c**, Quantification of Smad2 nuclear localization by automated immunofluorescence. Mv1Lu cells incubated in the buffers indicated in **b** were then treated with varying doses of TGF-β for 30 min at 37 °C. Following fixation and processing for standard immunofluorescence with Smad2 antibodies, the nuclear intensity of Smad2 minus the cytoplasmic intensity of Smad2 was quantified using DataViewer (v. 3.0) software (Cellomics) and graphed. Each datapoint represents data measured from the average of ≥ 200 cells ± SD. **d**, Model for TGF-β signal transduction and downregulation. TGF-β receptors internalize through two distinct endocytic pathways. Clathrin-dependent internalization into the early endosome is important for propagating signals, whereas the caveolin-1-positive lipid raft compartment is required for receptor degradation. The function of these pathways is dictated by the resident Smad and Smad-associated proteins, which are segregated between the two compartments as shown.

localization of SARA and the Smad7–Smurf2 ubiquitin ligase complex, which targets the receptors for degradation[25]. Analysis of SARA revealed extensive co-localization with the EEA1- and Rab5-positive early endosome as previously reported[27,29,30] (Fig. 4a and data not shown), but not Rab9, which marks the late endosome (data not shown) or caveolin-1 (Fig. 4a). In contrast, Smad7–Smurf2 complexes co-localized extensively with caveolin-1, but not EEA1 or SARA (Fig. 4b and data not shown). Thus, SARA and Smad7–Smurf2 are localized in different compartments.

SARA interacts with over-expressed TGF-β receptors in the absence of its FYVE domain[20], suggesting that in addition to its localization in the early endosome, a pool of SARA binds TGF-β receptors at the plasma membrane. To examine this, we analysed the interaction of endogenous SARA and TGF-β receptors at 4 °C (a temperature which prevents internalization) or at 37 °C. At either temperature, similar amounts of receptor complexes co-precipitated with SARA, indicating that SARA associates with receptors at the plasma membrane (Fig. 4c). We also tested R1B cells (which lack TβRI) and R1B-C10 (a R1B line that stably expresses ectopic TβRI) and observed that SARA co-precipitated with receptors in both cases (Fig. 4D). Alternatively, Smad7 bound only to receptor complexes in the presence of TβRI, supporting previous conclusions[23,25]. We conclude that SARA can associate with TβRII alone at the cell surface, whereas Smad7 interacts with the receptor complex through TβRI.

Smad7–Smurf2 targets raft-bound receptors for degradation. The co-localization of Smad7–Smurf2 with caveolin-1 suggested that this ubiquitin ligase complex preferentially targets TGF-β receptors in the raft compartment. To test this, we first analysed association of Smad7 with receptors, either in the absence or presence of wild type or catalytically inactive Smurf2 (Smurf2^{C716A}). Smad7-bound receptors were restricted to the raft compartment (Fig. 5a) and Smurf2 strongly reduced Smad7-bound receptors in rafts, whereas Smurf2^{C716A} enhanced their levels. We also examined interactions in Mv1Lu cells and observed that endogenous Smad7 preferentially associated with receptors in the raft compartment (Fig. 5b). Furthermore, interfering with proteasome activity increased both total and Smad7-bound receptors in the raft fraction. Thus, Smad7–Smurf2 targets raft-bound receptors.

Caveolin is associated with rafts and can regulate raft trafficking. The association of Smad7–Smurf2 with raft-bound receptors and the dependence of receptor turnover on raft function therefore suggested that caveolin might regulate receptor turnover. To assess this, we examined receptor turnover in 293T cells, which do not express detectable levels of caveolin-1 (ref. 31; G. Di G, C. Le R., A. G. and J. W., unpublished results). In control cells, the $t_{1/2}$ of the receptors was 6 h, with 40% of receptors still present by 12 h (Fig. 5c). However, in caveolin-1 expressing cells receptor half-life was reduced to 4 h and only 10% remained at 12 h. We next examined whether caveolin-1 and Smad7–Smurf2 can co-operate to further downregulate TGF-β receptors. To do this we chased cell surface labelled receptors for 1 h and fractionated cell lysates into raft and non-raft compartments. Expression of caveolin-1 or Smurf2 caused increased turnover of the receptor and co-expression of both proteins caused an even greater loss (Fig. 5d), suggesting that caveolin-1 can co-operate with Smad7–Smurf2 to enhance receptor degradation. These results indicate that caveolin-1 can cooperate with Smad7–Smurf2 complexes to target raft-bound receptors for degradation.

SARA and Smad7–Smurf2 regulate the fate of TGF-β receptors. The observation that SARA and Smad7 show mutually exclusive localization to the EEA1 or the caveolin positive compartments respectively suggests that the intracellular fate of receptors may be affected by their association with SARA or Smad7–Smurf2. To assess this, we used the model system of 293T cells overexpressing TβRII and TβRI. In the absence of transfected Smad7–Smurf2, the $t_{1/2}$ of receptors was about 8 h and was reduced to approximately 3 h in their presence (Fig. 6a, b). This enhancement was blocked by Nystatin treatment (Fig. 6b), confirming that lipid raft integrity is important for Smad7–Smurf2-mediated turnover of TGF-β receptors. When SARA was co-expressed with Smad7–Smurf2, receptor stability was close to control levels (Fig. 6a, b). This was dependent on the association of SARA with the receptor, as a mutant of SARA missing the receptor-binding domain (Δ750–1323) was unable to stabilize the receptors (Fig. 6c). Furthermore, a SARA mutant that cannot localize to endosomes[20] due to deletion of the FYVE domain (SARA$^{\Delta FYVE}$), was unable to prevent Smad7–Smurf2-dependent receptor degradation (Fig. 6c). Therefore, the ability of SARA to bind PtdIns(3)P through its FYVE domain can function to stabilize receptors and inhibit Smad7–Smurf2-dependent degradation through raft-dependent pathways.

Receptor compartmentalization regulates signal transduction. We have established that the clathrin-dependent pathway promotes TGF-β signal transduction, whereas the raft-caveolar pathway is important for downregulating signalling. Furthermore, partitioning of the receptor between raft and non-raft membranes is dynamic (Fig. 7a, i) and blocking clathrin-dependent endocytosis not only prevents entrance of receptors into the EEA1 compartment, but also results in accumulation of receptors in rafts (Fig. 7a, ii). Consequently, we considered the possibility that clathrin-dependent endocytosis might function to sequester receptors from the raft-caveolar pathway. If this were the case, we reasoned that the block in Smad activation caused by interfering with clathrin might be reversed by concomitantly interfering with rafts (Fig. 7a, iii). To test this hypothesis, we utilized potassium (K^+) depletion and Nystatin and examined Smad2 phosphorylation. Potassium depletion strongly suppressed receptor-dependent Smad2 phosphorylation, however, co-treatment with Nystatin restored phosphorylation to about 50% of untreated cells (Fig. 7b). Phosphorylation induces the nuclear accumulation of Smad2. Therefore, we also quantitatively analysed nuclear Smad2 levels. In control cells, TGF-β induced a dose-dependent accumulation of Smad2 in the nucleus (Fig. 7c) and although Nystatin had no effect, K^+-depletion completely blocked accumulation. Treatment of K^+-depleted cells with Nystatin restored TGF-β-dependent Smad2 nuclear accumulation. These results suggest that trafficking of receptors to the SARA and EEA1-positive early endosome functions to sequester receptors from rafts and caveolae, which negatively regulate the signal transduction pathway.

Discussion

In mammalian cells internalization of cell surface proteins occurs through both clathrin-dependent and independent pathways[1]. Signal transduction can continue from the clathrin-coated endosomal pathway after internalization[2–4], but the pathway is also important for down-regulating receptors. For example, epidermal growth factor (EGF) receptors cluster within minutes of ligand addition, are internalized through clathrin-dependent pathways and are ubiquitinated through the ubiquitin ligase c-cbl[45], which tags the receptor for lysosomal degradation. Clathrin-independent endocytosis through lipid raft and caveolar pathways can also occur by both dynamin-dependent and independent processes[6,43]. The IL-2 receptor, for instance, appears to internalize exclusively through a non-clathrin pathway that involves lipid rafts[46] and caveolin-containing vesicles have been shown to mediate internalization of the SV40 virus and AMF receptor[11,16,47]. However, it has been unclear how important raft and caveolar internalization are in regulating signal transduction receptors. Here we show that TGF-β Ser-Thr kinase receptors internalize through the classical clathrin-dependent pathway, as well as a raft-caveolin route (Fig. 7d) with the former pathway facilitating Smad activation[27–30] and the latter mediating receptor degradation. Furthermore, unlike classical ligand-dependent trafficking and downregulation, we found that TβRII internalization was

unaffected by ligand stimulation. Thus, we propose that in the Ser-Thr kinase receptor system, ligands do not regulate trafficking but rather act to recruit the type I receptor and stabilize heterotetrameric receptor complexes during constitutive trafficking events. The activated type I receptor subsequently signals in the EEA1-positive endosome by phosphorylating Smad2 recruited by SARA, or directing degradation through lipid raft pathways by binding Smad7–Smurf2 complexes.

We have shown that TGF-β receptors constitutively traffic into different endocytic pathways. Although clathrin-dependent trafficking may be mediated by a dileucine-based motif in TβRII[26] that would bind to the clathrin adaptor protein AP-2, it remains unclear what mediates raft partitioning and localization in caveolar vesicles. Internalization into different endocytic compartments serves to bring the receptor to distinct Smads and Smad-associated proteins. In the clathrin pathway the Smad2 anchoring protein SARA is bound to receptors at the plasma membrane, but is highly enriched in the early endosome and little if any is found in caveolin-positive structures. In contrast, Smad7–Smurf2 complexes co-localize with caveolin, but not the EEA1-positive compartment. Thus, we propose that Smad signalling components segregate in the two internalization pathways and confer distinct activities to these compartments in the regulation of TGF-β signalling.

Separation of Smad signalling components between endocytic pathways is likely determined by the differential composition of the lipid bilayer in the two compartments. SARA localization to the early endosome is dependent on its FYVE domain[29,30], which binds PtdIns(3)P, a phospholipid highly enriched in the EEA1-positive endosome, whereas the unique cholesterol- and sphingolipid-rich composition of lipid rafts likely dictates the preferential association of Smad7–Smurf2 complexes with this compartment. Nedd4, another C2-WW-HECT ubiquitin ligase that induces degradation of epithelial sodium channels (ENaC), is also enriched in lipid rafts[48], suggesting that endocytic routes utilized by lipid rafts may represent a new compartment for regulating ubiquitin-dependent degradation of membrane proteins by C2-WW-HECT domain ubiquitin ligases.

Our analysis of TGF-β receptor turnover defined the raft-caveolin compartment as an important negative regulator of TGF-β signalling, and ectopic expression of caveolin-1 in 293T cells enhances receptor turnover and co-operates with Smad7–Smurf2 to cause rapid receptor loss from the raft compartment. However, it is important to note that in the absence of caveolin-1 expression, Smad7 was still bound to TGF-β receptors in the raft compartment and Smad7–Smurf2-dependent receptor turnover was inhibited by Nystatin. These results suggest that although caveolin can facilitate receptor turnover, raft-dependent degradation can occur in its absence, consistent with the notion that trafficking of raft components occurs in the absence of caveolin expression[6]. How the dynamics of raft levels and caveolin expression might affect TGF-β receptor trafficking and cellular responsiveness will be an interesting area for future investigation.

Why is trafficking of TGF-β receptors into clathrin-dependent pathways critical for activation of Smads? The enrichment of SARA in the early endosome might suggest that clathrin-dependent endocytosis brings the receptor to SARA-bound Smad2. However, endogenous SARA is bound to the receptor at the plasma membrane, so receptors need not move into the early endosome to access Smad2-bound SARA. In addition, it has been suggested that inhibiting the clathrin pathway in HeLa cells does not affect TGF-β signalling[44]. Thus, the observation that Nystatin treatment rescues the block in Smad activation caused by K^+-depletion suggests an alternative possibility — that clathrin-dependent internalization functions to sequester receptors away from the rafts and caveolin, which can inhibit the receptor directly through caveolin-1 binding to TβRI or through Smad7–Smurf2-dependent ubiquitination. The shift of receptors into the raft compartment that occurs upon inhibiting clathrin-dependent endocytosis supports this model. Also in support is the observation that overexpressed SARA prevented Smad7–Smurf2-dependent degradation and that this required its FYVE domain, indicating that the anchoring of SARA to the endosomal membrane can protect receptors. Hrs, another FYVE domain-containing protein may also function in this way as it also binds TGF-β receptors and Smads[49]. Together, these results suggest that the early endosome represents a signalling centre that functions to both sequester active receptor complexes from rafts and caveolin and to promote access to the Smad2 substrate through SARA. Consequently, the requirement for clathrin-dependent endocytosis in different cell types may depend in part on the propensity of receptors to enter rafts when this pathway is blocked. Furthermore, lipid rafts inhibit a number of other classes of receptors, including the EGF and platelet-derived growth factor (PDGF) tyrosine kinase receptors and Hrs (which also binds receptor tyrosine kinases) can sequester EGF receptors in the early endosome[50]. Therefore retention of receptors in the early endosome through the action of FYVE domain proteins may function in other signalling systems to direct receptors away from the inhibitory activity of lipid rafts. It will be interesting to see how trafficking through the EEA1-positive early endosome and lipid raft-dependent pathways functions to control signal transduction and down-regulation in other receptor systems. □

Methods

Cell lines, antibodies and cDNA

Mv1Lu, R1B and HepG2 cells were grown in MEM media supplemented with non-essential amino acids and 10% foetal bovine serum (FBS). R1B cells stably transfected with a pMEP4 plasmid containing the cDNA for TβRI or Mv1Lu cells stably transfected with pMEP4 containing cDNA encoding HA-tagged TβRII (HAT cells) were passaged in media supplemented with 0.3 mg/ml Hygromycin. HEK 293T cells were passaged in DMEM-10%FBS. Anti-HA (12CA5; Boehringer, Quebec, Canada), anti-Myc (9E10 ascites; Developmental Studies Hybridoma Bank, Iowa, IA), anti-HA polyclonal (Santa Cruz Technologies, Santa Cruz, CA), mouse anti-Fab HA (Babco, Richmond, CA), anti-TβRII polyclonal (C16; Santa Cruz), monoclonal anti-Smad2, mouse anti-caveolin 1, rabbit anti-caveolin-1 pAb, mouse anti-EEA1, monoclonal anti-p62, monoclonal anti-Rab11 (Transduction Laboratories, San Jose, CA) and polyclonal anti-PhosphoSmad2 (UBI, Lake Placid, NY) antibodies were used as instructed. Polyclonal rabbit anti-SARA antibodies were raised to the peptide corresponding to amino acids 20–36 of human SARA (Research Genetics, Inc., Ontario, Canada), goat anti-SARA antibodies (Santa Cruz) and rabbit anti-Smad7 antibodies were used as described[25]. The Fab fragments used in the immunofluorescence studies were prepared from anti-HA polyclonal antibody (Santa Cruz). Secondary antibodies (IgG or Fab fragments, Jackson Laboratories Inc., West Grove, PA) used in the immunofluorescence microscopy studies were used as suggested and secondary antibodies used in electron microscopy were purchased from Auriom Electron Microscopy Sciences (Washington, PA) and from Amersham Pharmacia Biotech (Piscataway, NJ). pcDNA3 wild-type dynamin (WT) and dominant negative dynamin (K44A) were generously provided by S. Egan. pEGFP Eps15-DIII and DIIIΔ2 were a generous gift from A. Benmerah and cDNA encoding caveolin-1 was a generous gift from M. P. Lisanti and B. Razani.

K^+ depletion, Nystatin and methyl β-cyclodextrin treatment

Clathrin-dependent endocytosis was delayed by K^+ depletion. Briefly, cells were incubated in DMEM:water (1:1) for 5 min at 37 °C followed by incubation in minimal media (20 mM Hepes at pH 7.5, 140 mM sodium chloride, 1 mM calcium chloride, 1 mM magnesium sulphate, 5.5 mM glucose and 0.5% BSA) for 1 h at 37 °C. Control cells were incubated in minimal media supplemented with 10 mM potassium chloride. Cholesterol depletion, which affects caveolae-mediated endocytosis, was carried out by incubating cells in 50 μg ml^{-1} of Nystatin (Sigma) or 2.5 mM methyl β-cyclodextrin for 1 h at 37 °C.

Immunofluorescent microscopy

For subcellular localization studies, Mv1Lu cells were plated on gelatin-coated Permanox chamber slides (Nunc, Rochester, NY) and transfected with the indicated constructs by the calcium phosphate precipitation method. Fixation, permeabilization, and reaction with the primary and secondary antibodies were described previously[25]. Images were obtained using the Olympus 1X70 (Ontario, Canada) inverted microscope equipped with fluorescence optics and Deltavision deconvolution microscopy software (Applied Precision, Issaquah, WA). Receptor internalization studies were carried out as described[26]. Briefly, Mv1Lu cells expressing extracellularly HA-tagged TβRII were incubated with rabbit anti-HA antibodies or Fab fragments in KRH-0.5% BSA for 2 h at 4 °C. Following 3 washes with buffer, cells were incubated with Cy3-conjugated goat anti-rabbit Fab fragments for 1 h at 4 °C. Cells were then washed, incubated with or without 0.5 nM TGF-β at 4 °C or 37 °C, fixed and incubated with appropriate antibodies as described above. For TGF-β trafficking studies, cells were incubated with biotinylated TGF-β, followed by Cy3-conjugated streptavidin as described for antibody studies. For acid wash experiments, cells were washed for 10 min at 4 °C with a 150 mM soduim chloride, glycinate buffer (at pH 2.5). For the triple label experiments, mouse Fab anti-HA, mouse anti-EEA1 and the rabbit anti-caveolin-1 were detected with goat anti-mouse Cy3-conjugated Fab fragments, anti-mouse FITC-conjugated Fc-specific antibody, and Cy5-conjugated anti-rabbit antibody, respectively.

Automated immunofluorescence microscopy was carried out in 96 well plates and visualized by using an ArrayScan II system (Cellomics, Pittsburgh, PA) and quantified using DataViewer (v. 3.0) software.

Electron microscopy

Pre-embedding immunogold labelling for HA-tagged TGF-β receptors was carried out as described above using anti-rabbit or anti-mouse anti–HA antibodies followed by goat anti-rabbit antibody conjugated to 10 nm colloidal gold or by goat anti-mouse antibody conjugated to 6 nm colloidal gold, respectively. One half of the samples were processed for optimal morphology of cell membranes and the other half was prepared for post-embedding immunogold labelling. The samples processed for optimal morphology were fixed with 2% glutaraldehyde in phosphate buffer, post-fixed with potassium ferrocyanide reduced osmium tetroxide and embedded in epon. Thin sections were contrasted with uranyl acetate and lead citrate. Samples for post-embedding labelling were fixed in 2% paraformaldehyde and 0.2% glutaraldehyde in phosphate buffer or in 4% paraformaldehyde and 0.5% glutaraldehyde in phosphate buffer and embedded in LR White or Lowicryl K4M (Polysciences, Warrington PA), respectively. Thin sections were incubated in primary mouse or primary rabbit antibody to caveolin-1 and the primary antibodies were detected with goat anti-mouse antibody conjugated to 6 nm colloidal gold or with goat anti-rabbit antibody conjugated to 10 nm colloidal gold, respectively. Sections were then contrasted with uranyl acetate and images obtained by transmission electron microscopy on a Phillips 400 electron microscope at 80 kV or a Hitachi 7000 electron microscope at 75 kV.

Affinity labelling

Mv1Lu, R1B, R1B cells overexpressing TβRI or transfected 293T cells, were incubated with 250 pM [^{125}I]TGF-β1 in KRH-0.5%BSA at 4 °C for 2 h or at 37 °C for 1 h, and receptors were cross-linked to ligand with DSS as described previously[20]. Cell lysates were either immunoprecipitated with anti-TβRII, anti-SARA or anti-Smad7 antibodies, and receptors were visualized by SDS–polyacrylamide gel electrophoresis and autoradiography. Receptor levels were quantified using a phosphorimager (Molecular Dynamics).

Detergent-free purification of raft-rich membrane fractions

MvLu1, HAT or 293T cells were grown to confluence in 150-mm diameter plates and affinity- labelled as described above. After 1 h at 37 °C in media supplemented with 0.2% FBS, the cells were subjected to sucrose density centrifugation as described[36].

Immunoprecipitation and immunoblotting

Mv1Lu or 293T cells were transiently transfected using the calcium phosphate precipitation method. Cell were lysed in 0.5% TNTE (50 mM Tris at pH 7.4, 150 mM sodium chloride, 1 mM EDTA, 0.5% Trition X-100), and immunoprecipitations were carried out using the antibodies described above. After absorption of the antibody to either protein G or A–Sepharose, the precipitates were washed five times with TNTE containing 0.1% Triton X-100, subjected to SDS-PAGE, transferred onto nitricellulose and immunoblotted with the appropriate antibodies. Detection was achieved using horseradish peroxidase-conjugated goat anti-mouse or goat anti-rabbit secondary antibodies and chemiluminescence (Amersham).

Transcriptional response assay

HepG2 cells were transiently transfected with Fast2 (FoxH1), βgal and A3-Lux reporter constructs. Twenty-four hours after transfection cells were incubated for 6 h in control media, media lacking potassium chloride or media supplemented with Nystatin as described above with or without 100 pM TGF-β. Luciferase activity was measured using the luciferase assay system (Promega, Madison, WI) in a Berthold Lumat LB 96V luminometer and normalized to β-galactosidase activity. For dominant negative mutant studies, HepG2 cells were transiently transfected with Fast2 (FoxH1), βgal and A3-Lux reporter constructs and dynamin (wild type or K44A), Eps15 control (DIIIΔ2) or DIII. Twenty-four hours after transfection cells were serum starved and incubated in 100 pM TGF-β for 16 h.

RECEIVED 4 OCTOBER 2002; REVISED 9 JANUARY 2003; ACCEPTED 26 FEBRUARY 2003; PUBLISHED 28 APRIL 2003.

1. Gruenberg, J. The endocytic pathway: a mosaic of domains. *Nature Rev. Mol. Cell Biol.* **2,** 721–730 (2001).
2. Baass, P. C., Di Guglielmo, G. M., Authier, F., Posner, B. I. & Bergeron, J. J. M. Compartmentalized signal transduction by tyrosine kinases. *Trends Cell Biol.* **5,** 465–470 (1995).
3. Di Fiore, P. P. & De Camilli, P. Endocytosis and signaling. an inseparable partnership. *Cell* **106,** 1–4 (2001).
4. McPherson, P. S., Kay, B. K. & Hussain, N. K. Signaling on the endocytic pathway. *Traffic* **2,** 375–384 (2001).
5. Katzmann, D. J., Babst, M. & Emr, S. D. Ubiquitin-dependent sorting into the multivesicular body pathway requires the function of a conserved endosomal protein sorting complex, ESCRT-I. *Cell* **106,** 145–155 (2001).
6. Sharma, P., Sabharanjak, S. & Mayor, S. Endocytosis of lipid rafts: an identity crisis. *Sem. in Cell Dev. Biol.* **13,** 205–214 (2002).
7. Anderson, R. G. & Jacobson, K. A role for lipid shells in targeting proteins to caveolae, rafts, and other lipid domains. *Science* **296,** 1821–1825 (2002).
8. Simons, K. & Toomre, D. Lipid rafts and signal transduction. *Nature Rev. Mol. Cell Biol.* **1,** 31–39 (2000).
9. Anderson, R. G., Kamen, B. A., Rothberg, K. G. & Lacey, S. W. Potocytosis: sequestration and transport of small molecules by caveolae. *Science* **255,** 410–411 (1992).
10. Razani, B., Schlegel, A. & Lisanti, M. P. Caveolin proteins in signaling, oncogenic transformation and muscular dystrophy. *J. Cell Sci.* **113,** 2103–2109 (2000).
11. Pelkmans, L., Kartenbeck, J. & Helenius, A. Caveolar endocytosis of simian virus 40 reveals a new two-step vesicular-transport pathway to the ER. *Nature Cell Biol.* **3,** 473–483 (2001).
12. Nichols, B. J. A distinct class of endosome mediates clathrin-independent endocytosis to the Golgi complex. *Nature Cell Biol.* **4,** 374–378 (2002).
13. Le, P. U., Guay, G., Altschuler, Y. & Nabi, I. R. Caveolin-1 is a negative regulator of caveolae-mediated endocytosis to the endoplasmic reticulum. *J. Biol. Chem.* **277,** 3371–3379 (2002).
14. Smart, E. J. *et al.* Caveolins, liquid-ordered domains, and signal transduction. *Mol. Cell Biol.* **19,** 7289–7304 (1999).
15. Prevostel, C., Alice, V., Joubert, D. & Parker, P. J. Protein kinase Cα actively downregulates through caveolae- dependent traffic to an endosomal compartment. *J. Cell Sci.* **113,** 2575–2584 (2000).
16. Roy, S. *et al.* Dominant-negative caveolin inhibits H-Ras function by disrupting cholesterol-rich plasma membrane domains. *Nature Cell Biol.* **1,** 98–105 (1999).
17. Massague, J. TGF-β signal transduction. *Annu Rev Biochem* **67,** 753–791 (1998).
18. Wrana, J. L., Attisano, L., Wieser, R., Ventura, F. & Massague, J. Mechanism of activation of the TGF-β receptor. *Nature* **370,** 341–347 (1994).
19. Miyazono, K., ten Dijke, P. & Heldin, C. H. TGF-β and signaling by Smad proteins. *Adv. Immunol.* **75,** 115–157 (2000).
20. Tsukazaki, T., Chiang, T. A., Davison, A. F., Attisano, L. & Wrana, J. L. SARA, a FYVE domain protein that recruits Smad2 to the TGF-β receptor. *Cell* **95,** 779–791 (1998).
21. Hayashi, H. *et al.* The MAD-related protein Smad7 associates with the TGF-β receptor and functions as an antagonist of TGF-β signaling. *Cell* **89,** 1165–1173 (1997).
22. Imamura, T. *et al.* Smad6 inhibits signalling by the TGF-β superfamily. *Nature* **389,** 622–626 (1997).
23. Nakao, A. *et al.* Identification of Smad7, a TGF-β-inducible antagonist of TGF-β signalling. *Nature* **389,** 631–635 (1997).
24. Ebisawa, T. *et al.* Smurf1 interacts with transforming growth factor-beta type I receptor through Smad7 and induces receptor degradation. *J. Biol. Chem.* **276,** 12477–12480 (2001).
25. Kavsak, P. *et al.* Smad7 binds to Smurf2 to form an E3 ubiquitin ligase that targets the TGF β receptor for degradation. *Mol. Cell* **6,** 1365–1375 (2000).
26. Ehrlich, M., Shmuely, A. & Henis, Y. I. A single internalization signal from the di-leucine family is critical for constitutive endocytosis of the type II TGF-β receptor. *J. Cell Sci.* **114,** 1777–1786 (2001).
27. Hayes, S., Chawla, A. & Corvera, S. TGF β receptor internalization into EEA1-enriched early endosomes: role in signaling to Smad2. *J. Cell Biol* .**158,** 1239–1249 (2002).
28. Penheiter, S. G. *et al.* Internalization-dependent and -independent requirements for transforming growth factor β receptor signaling via the Smad pathway. *Mol. Cell Biol.* **22,** 4750–4759 (2002).
29. Itoh, F. *et al.* The FYVE domain in Smad anchor for receptor activation (SARA) is sufficient for localization of SARA in early endosomes and regulates TGF-β-Smad signalling. *Genes Cells* **7,** 321–331 (2002).
30. Panopoulou, E. *et al.* Early endosomal regulation of Smad-dependent signaling in endothelial cells. *J. Biol. Chem.* **4,** 18046–18052 (2002).
31. Razani, B. *et al.* Caveolin-1 regulates transforming growth factor (TGF)-β-SMAD signaling through an interaction with the TGF-β type I receptor. *J. Biol. Chem.* **276,** 6727–6738 (2001).
32. Zwaagstra, J. C., El-Alfy, M. & O'Connor-McCourt, M. D. Transforming growth factor (TGF)-β 1 internalization: modulation by ligand interaction with TGF-β receptors types I and II and a mechanism that is distinct from clathrin-mediated endocytosis. *J. Biol. Chem.* **276,** 27237–27245 (2001).
33. de Renzis, S., Sonnichsen, B. & Zerial, M. Divalent Rab effectors regulate the sub-compartmental organization and sorting of early endosomes. *Nature Cell. Biol.* **4,** 124–133 (2002).
34. Sanchez, P., De Carcer, G., Sandoval, I. V., Moscat, J. & Diaz-Meco, M. T. Localization of atypical protein kinase C isoforms into lysosome- targeted endosomes through interaction with p62. *Mol. Cell. Biol.* **18,** 3069–3080 (1998).
35. Rubino, M., Miaczynska, M., Lippe, R. & Zerial, M. Selective membrane recruitment of EEA1 suggests a role in directional transport of clathrin-coated vesicles to early endosomes. *J. Biol. Chem.* **275,** 3745–3748 (2000).
36. McCabe, J. B. & Berthiaume, L. G. N-terminal protein acylation confers localization to cholesterol, sphingolipid-enriched membranes but not to lipid rafts-caveolae. *Mol. Biol. Cell* **12,** 3601–3617 (2001).
37. Rodal, S. K. *et al.* Extraction of cholesterol with methyl-beta-cyclodextrin perturbs formation of clathrin-coated endocytic vesicles. *Mol. Biol. Cell* **10,** 961–974 (1999).
38. Subtil, A. *et al.* Acute cholesterol depletion inhibits clathrin-coated pit budding. *Proc. Natl Acad. Sci. USA* **96,** 6775–6780 (1999).
39. Ros-Baro, A. *et al.* Lipid rafts are required for GLUT4 internalization in adipose cells. *Proc. Natl Acad. Sci. USA* **98,** 12050–12055 (2001).
40. Torgersen, M. L., Skretting, G., van Deurs, B. & Sandvig, K. Internalization of cholera toxin by different endocytic mechanisms. *J. Cell Sci.* **114,** 3737–3747 (2001).
41. Benmerah, A. *et al.* AP-2-Eps15 interaction is required for receptor-mediated endocytosis. *J. Cell Biol.* **140,** 1055–1062 (1998).
42. Damke, H., Baba, T., Warnock, D. E. & Schmid, S. L. Induction of mutant dynamin specifically blocks endocytic coated vesicle formation. *J. Cell Biol.* **127,** 915–934 (1994).
43. Henley, J. R., Krueger, E. W., Oswald, B. J. & McNiven, M. A. Dynamin-mediated internalization of caveolae. *J. Cell Biol.* **141,** 85–99 (1998).
44. Lu, Z. *et al.* Transforming growth factor β activates Smad2 in the absence of receptor endocytosis. *J. Biol. Chem.* **277,** 29363–29368 (2002).
45. Levkowitz, G. *et al.* c-Cbl-Sli-1 regulates endocytic sorting and ubiquitination of the epidermal growth factor receptor. *Genes Dev.* **12,** 3663–3674 (1998).
46. Lamaze, C. *et al.* Interleukin 2 receptors and detergent-resistant membrane domains define a clathrin-independent endocytic pathway. *Mol. Cell* **7,** 661–671 (2001).
47. Anderson, H. A., Chen, Y. & Norkin, L. C. Bound simian virus 40 translocates to caveolin-enriched membrane domains, and its entry is inhibited by drugs that selectively disrupt caveolae. *Mol. Biol. Cell* **7,** 1825–1834 (1996).
48. Plant, P. J. *et al.* Apical membrane targeting of Nedd4 is mediated by an association of its C2 domain with annexin XIIIb. *J. Cell Biol.* **149,** 1473–1484 (2000).
49. Miura, S. *et al.* Hgs (Hrs), a FYVE domain protein, is involved in Smad signaling through cooperation with SARA. *Mol. Cell Biol.* **20,** 9346–9355 (2000).
50. Raiborg, C., Bache, K. G., Mehlum, A., Stang, E. & Stenmark, H. Hrs recruits clathrin to early endosomes. *EMBO J.* **20,** 5008–5021 (2001).

ACKNOWLEDGEMENTS
The authors wish to thank S. Hearn (Mount Sinai Hospital, Toronto, EM facilities), J. Mui and J. Bergeron and A. Vali (Anatomy Cell Biology, McGill Montreal, EM Centre) and S. Doyle (Microscopy Imaging Laboratory, University of Toronto, EM facilities) for their assistance with the electron microscopy studies. The authors would also like to thank J. Bergeron, H. Benchabane, P. Cameron, R. Rasmussen and P. Kavsak for helpful advice, S. Kulkarni for help with deconvolution microscopy and L. Attisano and P. Cameron for critical review of the manuscript as well as L. Black, M. Pye and the members of the Wrana lab for assistance. This work was supported by grants to J. L. W. from the CIHR and the National Cancer Institute with funds from the Terry Fox run. C. L. R. is a Postdoctoral Fellow of the CIHR and J.L.W. is an International Investigator of the HHMI and an Investigator of the CIHR. Supplementary information accompanies the paper on www.nature.com/naturecellbiology
Correspondence and requests for materials should be addressed to J. W.

COMPETING FINANCIAL INTERESTS
The authors declare that they have no competing financial interests.

Fig. S1. TGFβ receptors and biotinylated TGFβ co-localize to the EEA1 or Caveolin-1 positive compartment.

A) Mv1Lu cells not expressing cell surface HA-tagged TβRII were incubated with biotinylated TGFβ (b-TGFβ) followed by incubation with Cy3-conjugated streptavidin. Following fixation and permeabilization, cells were incubated with either anti-EEA1 or anti-Caveolin-1 antibodies and visualized by deconvolution immunofluorescence microscopy. Examples of co-localization of b-TGFβ with either EEA1 or Caveolin-1 are indicated with arrowheads.

B) Mv1Lu cells expressing HA-tagged TβRII were incubated with mouse anti-HA Fab fragments and b-TGFβ followed by FITC-conjugated donkey anti-mouse antibodies and Cy3-conjugated streptavidin at 4˚C, washed and allowed to internalize for 30 min at 37˚C. After fixation and permeabilization, cells were incubated with either anti-EEA1 or anti-Caveolin-1 antibodies and visualized by deconvolution immunofluorescence microscopy. As indicated in the key, the co-localization of receptors (αHA) and b-TGFβ is indicated in yellow and the triple stain of receptors, ligand and either Caveolin-1 (A) or EEA1 (B) is indicated in white.

Fig. S2. TGFβ receptors do not co-localize with the late endosomal compartment, but partially co-localize with the recycling compartment. Mv1Lu cells expressing HA-tagged TβRII were incubated with mouse anti-HA Fab fragments and Cy3-conjugated donkey anti-mouse antibodies at 4˚C, washed and allowed to internalize for 60 min at 37˚C. Post-fixation and permeabilization, cells were incubated with late endosomal marker, anti-p62 (A) or the recycling endosomal marker, anti-rab11 (B) antibodies and visualized by deconvolution immunofluorescence microscopy. Colocalization of TβRII and rab11 is indicated with yellow arrows.

Fig. S3. Ultrastructural and immunoelectron microscopy of TβRII.. Ultrastructural and immunoelectron microscopic analysis of TGFβ receptor trafficking was carried out in Mv1Lu cells expressing HA-tagged TβRII. Cells were incubated with rabbit anti-HA antibodies at 4˚C followed by goat anti-rabbit antibodies conjugated to 10 nm colloidal gold. Following incubation at 37˚C for 5 min, cells were fixed and processed for optimal morphology and visualized by electron microscopy (A and B). Labelled receptors in clathrin-coated pits and vesicles (solid arrow) and non-clathrin coated structures with the characteristics of caveolae (open arrows) are indicated For immunoelectron microscopy (C), cells in which receptors were labelled with 10 nm gold were incubated for 60 min at 37˚C and processed for post-embedding immunogold labelling with anti-caveolin-1 antibodies followed by secondary antibodies conjugated to 6 nm colloidal gold. Large arrowheads (C) indicate 10 nm gold-labelled TβRII and small arrowheads indicate 6 nm gold-labelled caveolin-1. Bars = 100 nm.

Fig. S4. Comparison of transferrin and TGFβ ligand internalization. Mv1Lu cells expressing HA-tagged TβRII were incubated in control media, media lacking KCl (-KCl) or media containing 50 μg/ml Nystatin. Following incubation with biotinylated transferrin (A) or TGFβ (B) followed by Cy3-conjugated strepavidin, cells were incubated at 37˚C for 15 min (A) or 30 min (B) and washed in either neutral buffer or acidic buffer (+acid wash) prior to processing for staining with anti-EEA1 antibodies and deconvolution immunofluorescence microscopy. Co-localization of ligand (red) and EEA1 (green) is shown in yellow. Note that K^+ depletion blocks transferrin internalization, does not block b-TGFβ internalization, but prevents colocalization of b-TGFβ with EEA1.

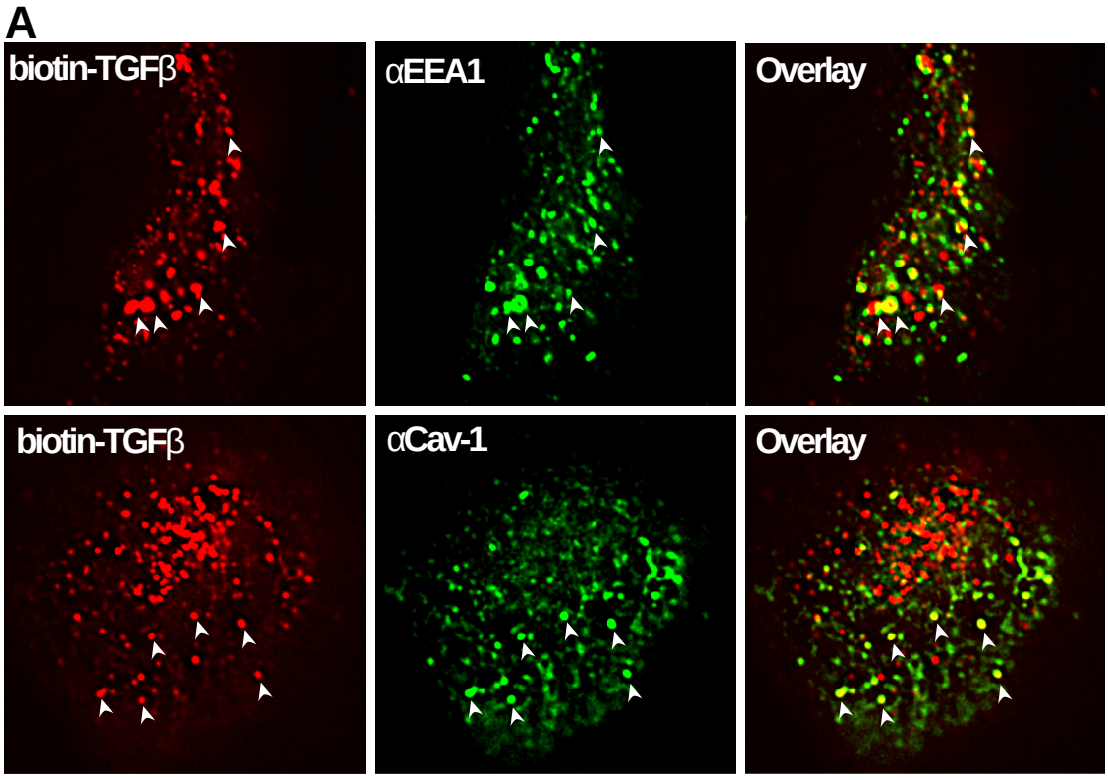

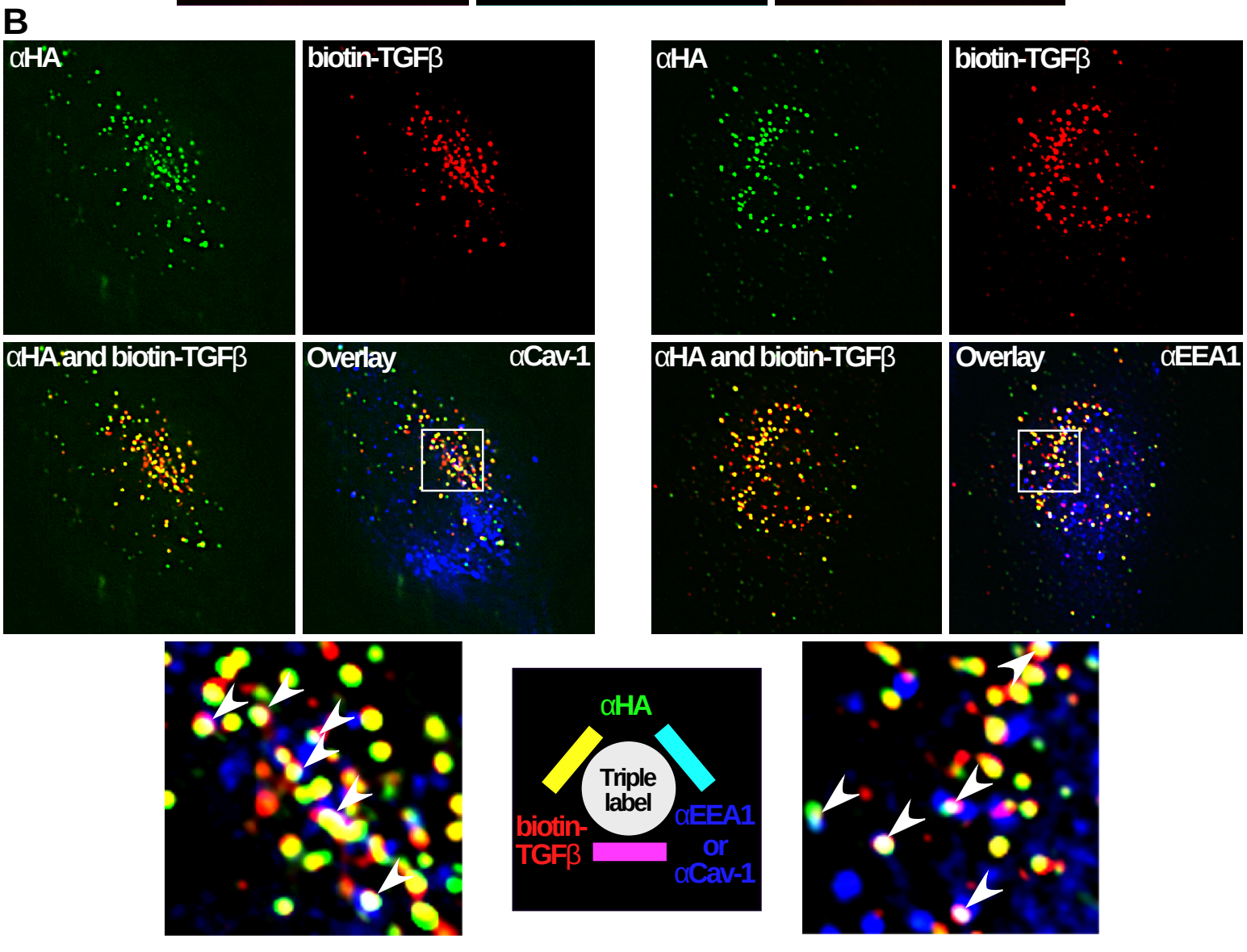

Supplemental Fig. S1. Di Guglielmo *et al.*

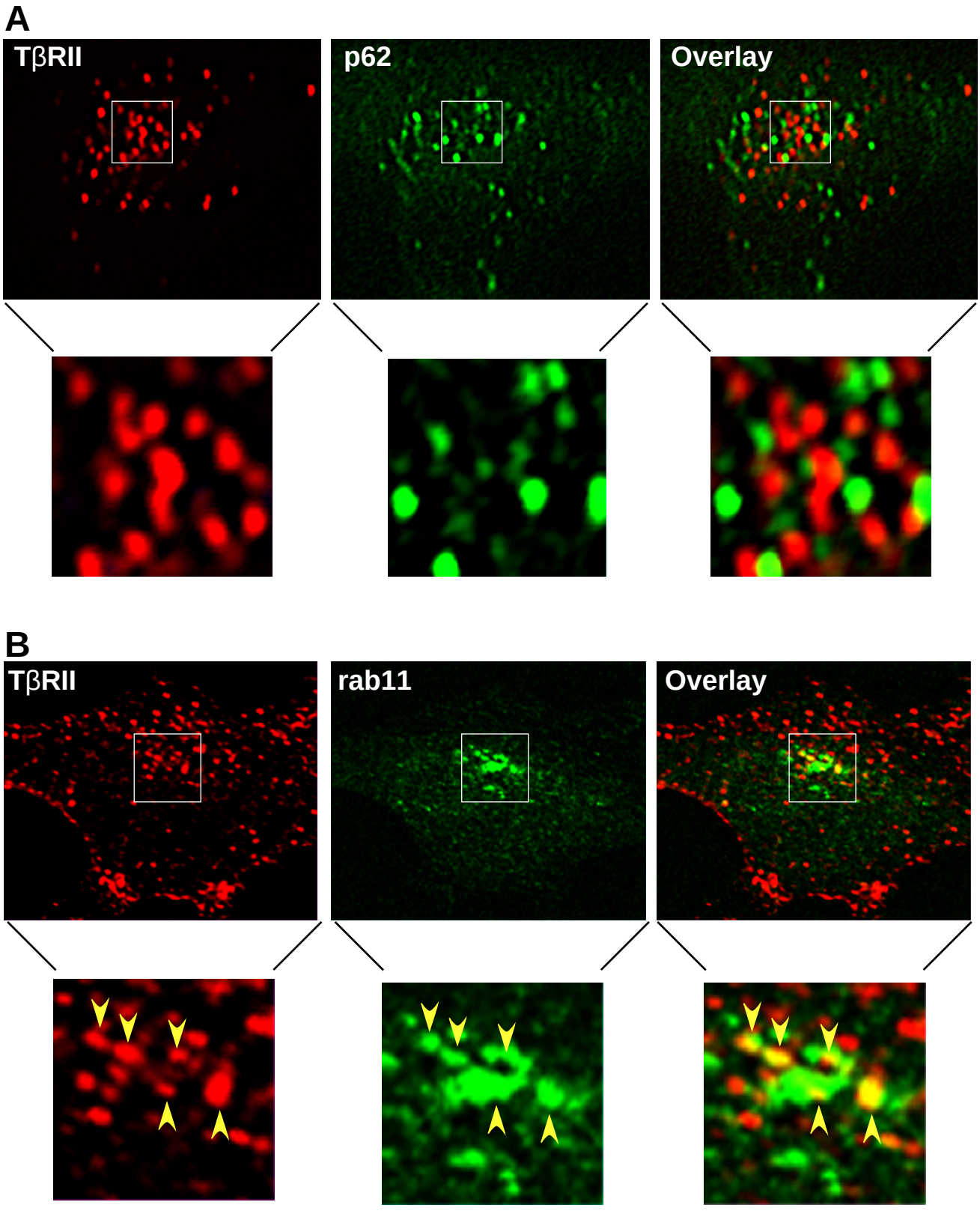

Supplemental Fig. S2. Di Guglielmo *et al.*

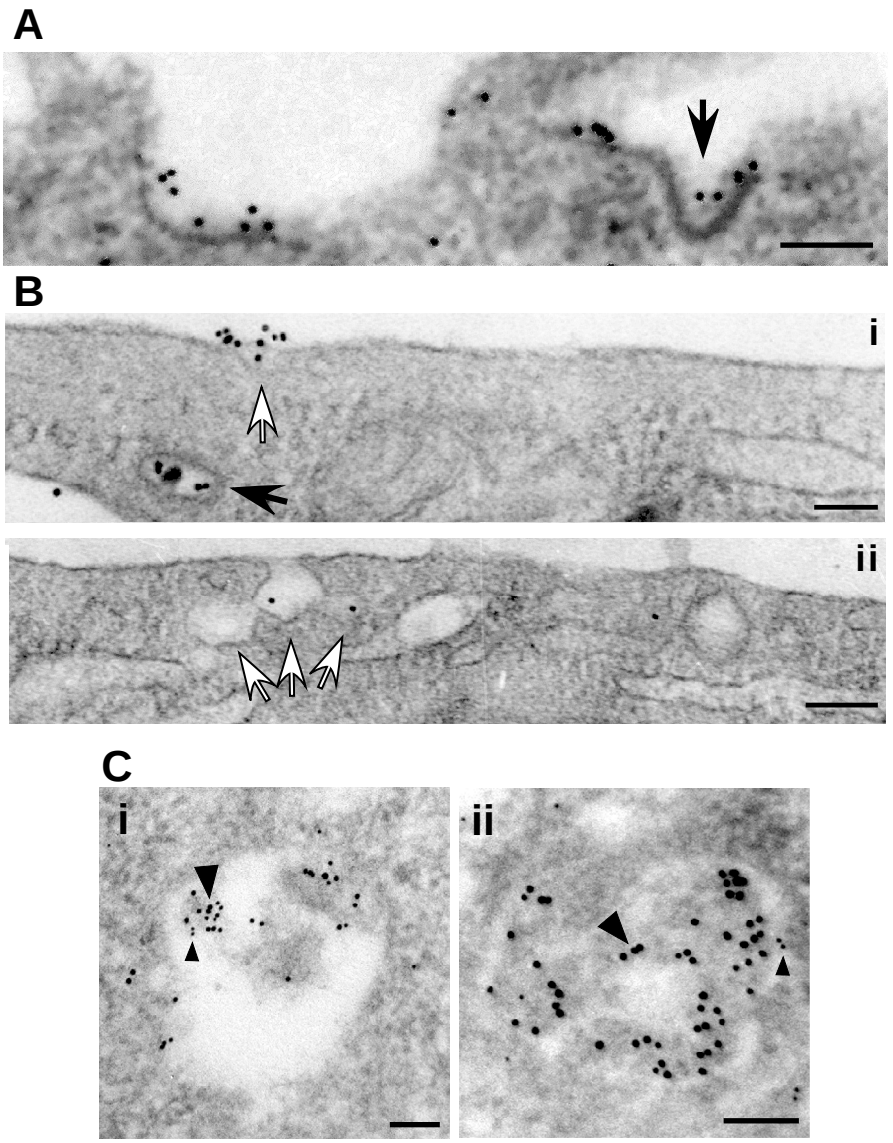

Supplemental Figure S3. Di Guglielmo *et al.*

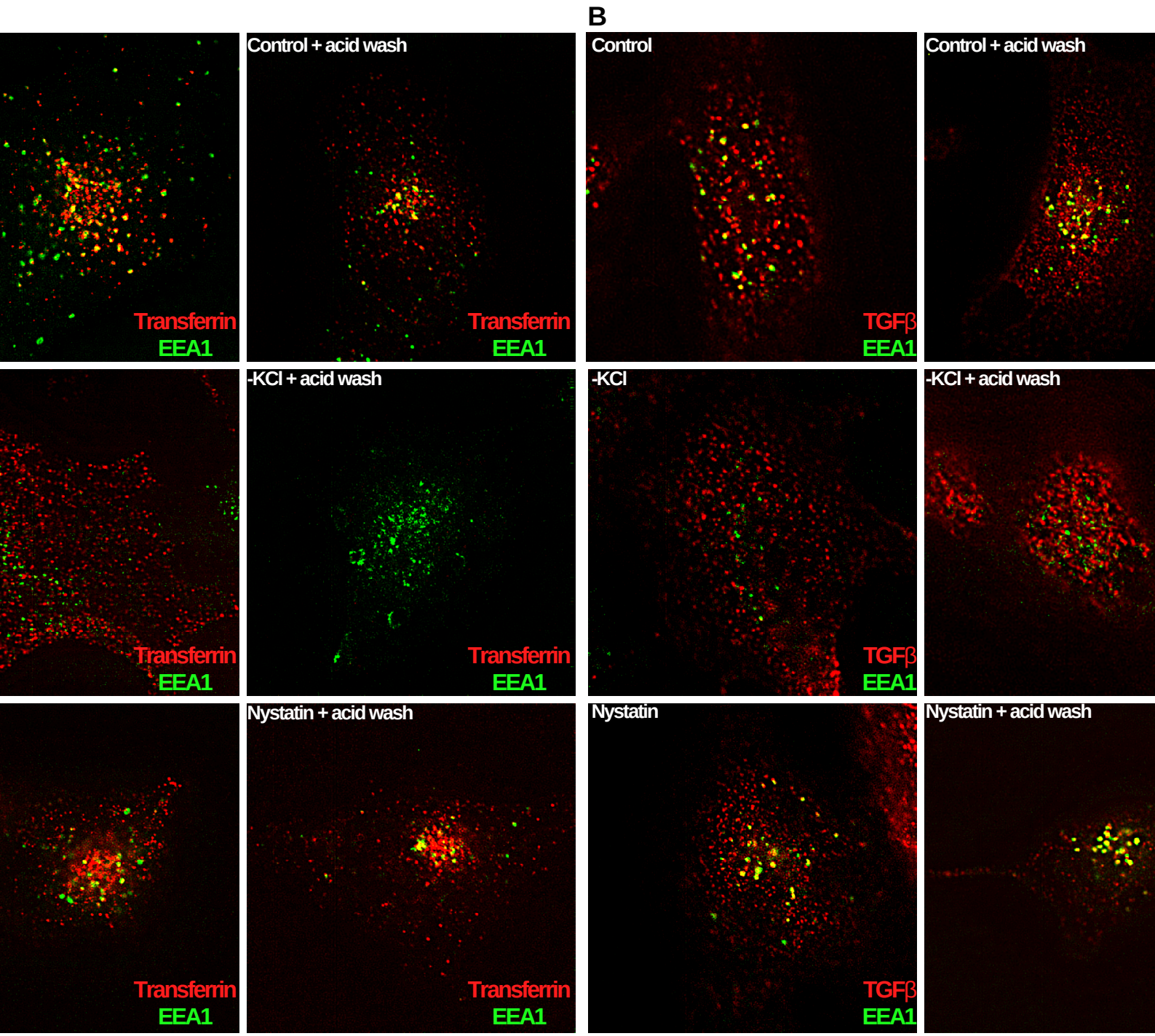

Supplemental Fig. S4. Di Gugliel

RETRACTION

Ramalingam, T. S., West, A. P., Lebron, J. A., Nangiana, J. S., Hogan, T. H., Enns, C. A. & Bjorkman, P. J. Binding to the transferrin receptor is required for endocytosis of HFE and regulation of iron homeostasis. *Nature Cell Biol.* **2,** 953–957 (2000).

In the course of repeating experiments described in the above paper, we have discovered that some of the confocal microscopy images presented in Figs 1 and 2 were inappropriately processed. A major point of the paper is that wild-type HFE expressed in HuTu-80 cells colocalizes with transferrin receptor (TfR) on the basolateral membrane and in intracellular transferrin (Tf)-positive endosomes, whereas a mutant form of HFE (HFE^{W81A}) that binds TfR with reduced affinity is localized mainly at the basolateral membrane and not in Tf-positive endosomes. In correctly processed images, we find HFE^{W81A} both at the basolateral membrane and in Tf-positive vesicles. Although the amount of HFE^{W81A} at the basolateral membrane versus HFE^{W81A} in intracellular vesicles is increased when compared with wild-type HFE (N.E. Tiangco and P.J.B., unpublished observations), the differences in HFE localization between cells expressing wild-type HFE and HFE^{W81A} are subtle. The paper also presents the results of western blots to measure ferritin levels in untransfected cells and cells expressing wild-type HFE, HFE^{W81A}, the hemochromatosis mutant HFE^{C260Y}, and wild-type and W81A forms of HFE to which the endosomal sorting sequence from the low-density lipoprotein receptor (LDLR) has been attached. Our current results are in agreement with the findings of the paper: that is, that ferritin levels are lower in HuTu-80 cells expressing wild-type HFE and wild-type HFE–LDLR than in untransfected HuTu-80 cells and in cells expressing HFE^{W81A}, HFE^{W81A}–LDLR or HFE^{C260Y} (A.-S. Zhang and C.A.E., unpublished observations). However, the differences between the present confocal images and the ones published with the paper require us to revise the conclusion that TfR binding by HFE is required for endocytosis of HFE and HFE-mediated regulation of ferritin levels, and we are therefore retracting the paper. We deeply regret any inconvenience this publication has caused for others.

The first author of this paper (T.S.R.) is not a cosignee of this retraction.

ERRATA

In Saucedo *et al.* (*Nature Cell Biol.* **5**, 566–571 (2003)), the first two sentences of the abstract should read:

Insulin signalling is a potent **stimulator** of cell growth and has been proposed to function, at least in part, through the conserved protein kinase TOR (target of rapamycin). Recent studies suggest that the tuberous sclerosis complex Tsc1–Tsc2 may couple insulin signalling to Tor activity.

rather than:

Insulin signalling is a potent **inhibitor** of cell growth and has been proposed to function, at least in part, through the conserved protein kinase TOR (target of rapamycin). Recent studies suggest a that the tuberous sclerosis complex Tsc1–Tsc2 may couple insulin signalling to Tor activity. This has also been corrected online.

In Guglielmo *et al.* (*Nature Cell Biol.* **5,** 410–421 (2003)), on p414, second column, line 9, the text should read:

Autoradiography (Fig. 1g) and quantitation (Fig. 1h) demonstrated that receptors were in the raft (55%) and non-raft fraction, which contained caveolin-1 or EEA1, respectively.

rather than:

Autoradiography (Fig. 1g) and quantitation (Fig. 1g) demonstrated that receptors were in the raft (55%) and non-raft fraction, which contained caveolin-1 or EEA1, respectively.

This has also been corrected online.

CORRIGENDUM

```
hDia2C          1 MEQPGAAASGAGGGSEEPGGGRSNKRSAGNRAANEEETKNKPKL-----------RDRITSFRKSTVKKEKPLIQHPIDSQVAMSEFPAA
hDia2B          1 MEQPGAAASGAGGGSEEPGGGRSNKRSAGNRAANEEETKNKPKLNIQIKTLADDVRDRITSFRKSTVKKEKPLIQHPIDSQVAMSEFPAA
mDia2           1 MERHRARALGRDSKSSRRKGLQSAPPAGPYEPGEKRPKLHLN-----IRTLTDDMLDKFASIRIPGSKKERPPLPHLKTVSGISDSSSLS
mDia1           1 MEPSGGGLGPGRGTRDKKKGRSPDELPATGGDGGKHKKFLER-----------------FTSMRIKKEKEKP----NSAHRNSSASYG
consensus       1 **..............  *.............. .. ....     .... ..............***.............. . ..

hDia2C         80 QPLYDERSLNLSEKEVLDLFEKMMEDMNLNEEKKAPLRNKDFTTKREMVVQYISATAKSIVGSKVTGGLKNSKHECTLSSQEYVHELRSG
hDia2B         91 QPLYDERSLNLSEKEVLDLFEKMMEDMNLNEEKKAPLRNKDFTTKREMVVQYISATAK-------SGGLKNSKHECTLSSQEYVHELRSG
mDia2          86 SETMENNPKALPESEVLKLFEKMMEDMNLNEDKKAPLREKDFGIKKEMVMQYINTASKTG----------SLRSSRQISPQEFLHELKMG
mDia1          68 DDPTAQSLQDISDEQVLVLFEQMLVDMNLNEEKQQPLREKDIVIKREMVSQYLHTSKAG-----------MNQKESSRSAMMYIQELRSG
consensus      91 ..............**.***.*..******.*..*** **.. *.***.**.. ....      .............*......**..*
```

In Gasman *et al.* (*Nature Cell Biol.* **5**, 195–204 (2003)), the correct sequence alignment in Fig. 1a should be:

Consequently, on page 197, the text in the right column, line 2, should read "... deletion of 11 (45–55 of hDia2B exon 12C and 156) ...". Similarly, the text on line 16 should read "... amino acids 45–55 of hDia2-12C ...". These changes do not significantly alter the conclusions and conceptual message of the paper. This has also been corrected online.